HHS Public Access

Author manuscript

Acta Neuropathol. Author manuscript; available in PMC 2017 May 01.

Published in final edited form as:

Acta Neuropathol. 2016 May ; 131(5): 687–707. doi:10.1007/s00401-016-1570-0.

Brain imaging of neurovascular dysfunction in Alzheimer's disease

Axel Montagne[1], **Daniel A. Nation**[2], **Judy Pa**[3], **Melanie D. Sweeney**[1], **Arthur W. Toga**[3], and **Berislav V. Zlokovic**[1]

[1]Zilkha Neurogenetic Institute and Department of Physiology and Biophysics, Keck School of Medicine, University of Southern California, Los Angeles, CA 90089, USA

[2]Department of Psychology, University of Southern California, Los Angeles, CA 90089, USA

[3]Department of Neurology, Institute for Neuroimaging and Informatics, University of Southern California, Los Angeles, CA 90089, USA

Abstract

Neurovascular dysfunction, including blood–brain barrier (BBB) breakdown and cerebral blood flow (CBF) dysregulation and reduction, are increasingly recognized to contribute to Alzheimer's disease (AD). The spatial and temporal relationships between different pathophysiological events during preclinical stages of AD, including cerebrovascular dysfunction and pathology, amyloid and tau pathology, and brain structural and functional changes remain, however, still unclear. Recent advances in neuroimaging techniques, i.e., magnetic resonance imaging (MRI) and positron emission tomography (PET), offer new possibilities to understand how the human brain works in health and disease. This includes methods to detect subtle regional changes in the cerebrovascular system integrity. Here, we focus on the neurovascular imaging techniques to evaluate regional BBB permeability (dynamic contrast-enhanced MRI), regional CBF changes (arterial spin labeling- and functional-MRI), vascular pathology (structural MRI), and cerebral metabolism (PET) in the living human brain, and examine how they can inform about neurovascular dysfunction and vascular pathophysiology in dementia and AD. Altogether, these neuroimaging approaches will continue to elucidate the spatio-temporal progression of vascular and neurodegenerative processes in dementia and AD and how they relate to each other.

Keywords

Alzheimer's disease; Neurovascular dysfunction; Blood–brain barrier; Cerebral blood flow; Magnetic resonance imaging

Introduction

Vascular contributions to dementia and Alzheimer's disease (AD) are increasingly recognized [115, 198]. It is estimated that up to 45 % of all dementias worldwide is wholly or partly due to age-related small vessel disease of the brain [188]. AD is characterized by

✉Berislav V. Zlokovic, zlokovic@usc.edu.

the presence of neurovascular dysfunction, inflammation, tau neurofibrillary tangles, amyloid-β (Aβ) plaques, neuronal loss and cognitive decline [198]. How these different pathologies relate to each other and contribute to cognitive decline, particularly during early stages of preclinical AD, and their exact role in the disease pathogenesis, remains, however, still debatable. Neuroimaging methods are currently used to aid in AD diagnosis by identifying structural and functional brain changes via magnetic resonance imaging (MRI) or positron emission tomography (PET), which was virtually impossible to assess in the living human brain until recently [115, 124]. Alongside to contributing to AD diagnostic confirmation, imaging can also inform differential diagnosis by identifying alternative and/or related pathologies, for instance cerebrovascular disorder and non-AD neurodegenerative diseases contributing to a complex spectrum of dementias.

Determining early AD pathophysiological changes has immediate prognostic importance during preclinical AD and mild cognitive impairment (MCI) stages. Only a fraction of MCI patients progress to clinical AD over 5–10 years, and a recent meta-analysis concluded that the majority of MCI patients will not progress to dementia even after 10 years follow-up [114]. Interestingly, over one-third of patients diagnosed with MCI at baseline may eventually return to normal cognition [66]. Therefore, during preclinical and MCI stages of AD it would be enormously beneficial to predict when and who will progress to AD, and have reliable and predictive neuroimaging biomarkers supporting conversion from preclinical and MCI stages to AD, and/or back from the MCI stage to a normal cognitive stage.

Recent technological advances in neuroimaging, including novel image acquisition sequences and pre- and post-processing analyses, now enable sensitive regional and quantitative measures of cerebrovascular functions and brain's structural and functional connectivity to be studied. For example, multiparametric neuroimaging approaches (i.e., dynamic-, functional-, and structural-MRI, and molecular PET imaging) are being used recently to evaluate neurovascular dysfunction in early dementia and AD including MRI methods to measure regional blood–brain barrier (BBB) permeability and cerebral blood flow (CBF) dysregulation, cerebral blood volume (CBV), cerebral metabolic rate of oxygen consumption ($CMRO_2$), microbleeding events, white matter connectivity, white matter lesions (WML), and regional brain atrophy, as well as PET imaging of BBB glucose transport and amyloid cerebrovascular pathology. Neuroimaging can offer enormous benefit to AD research and practice, particularly when applied longitudinally to elucidate regional and temporal developments of different pathologies, enable early detection of pathological and functional changes, inform novel treatment targets, and evaluate therapeutic efficacy. Here, we review neurovascular imaging approaches and examine how they can inform us about neurovascular dysfunction and vascular pathophysiology in AD and how they can potentially contribute to identify individuals at risk for dementia and AD.

Neurovascular dysfunction in AD

The etiology of late-onset sporadic AD is currently unknown, but mounting evidence suggests that cerebrovascular dysfunction contributes to AD etiology and progression [115, 198].

The neurovascular unit

The neurovascular unit (NVU) is comprised of vascular cells (endothelial cells, pericytes, vascular smooth muscle cells), glia (astrocytes, microglia, oligodendrocytes), and neurons that collectively underlie all functional responses of the central nervous system (CNS) [198]. Brain microvessels form a physical BBB that normally prevents macromolecules such as neuroactive peptides and proteins from entering the brain [199] unless they have specific carriers and/or receptors in brain endothelium [109, 197], which contrasts with the highly permeable vasculature in peripheral circulation [111]. Moreover, an intact BBB importantly regulates Aβ clearance from brain via receptor-mediated transport mechanisms in microvascular endothelium that control efflux of brain-derived Aβ from brain to circulation and influx and/or re-entry of circulating Aβ into the brain [109]. Brain endothelial cells are also able to regulate their own local coagulation environment within the brain microcirculation that is critical for normal capillary blood flow [186]. In AD, however, cerebrovascular dysfunction at the NVU including BBB breakdown, disrupted CBF, hypoperfusion, oligemia, and impaired vascular brain-to-blood clearance and blood-to-brain transport of Aβ contributes to disease pathophysiology [115, 198, 200].

Two-hit vascular hypothesis of AD

According to the two-hit vascular hypothesis, damage to brain microcirculation (*hit one*) in the aging brain, which may result from the effects of genetic risk factors, environmental factors, lifestyle or vascular risk factors such as hypertension, diabetes and/or hyperlipidemia, initiates a cascade of pathogenic events. This includes changes in BBB function such as BBB breakdown and increased permeability, and changes in brain perfusion including CBF dysregulation and reduction. BBB breakdown allows entry into the brain of blood-derived neurotoxic molecules (e.g., immunoglobulins, albumin, fibrinogen, and thrombin) and cells (e.g., erythrocytes, leukocytes, among others) that cause vascular pathology in brain parenchyma and can directly damage neurons [199]. Altogether, the vascular disruption contributes to the second hit (*hit two*), where increased Aβ accumulation in brain parenchyma and impaired clearance exerts neurotoxic effects on the brain leading to neurodegeneration and dementia [46]. Increasing number of studies recognize a synergistic relationship between BBB dysfunction and Aβ accumulation and neurofibrillary tangles, which initially form in the medial temporal lobe and hippocampus during the early stages of the disease before progressing to the neocortex [124]. Specifically, inadequate cerebral perfusion can promote Aβ accumulation and neurofibrillary tangles, and the neurotoxic effects of Aβ in turn impair vascular function, such as endothelial function and neurovascular coupling, and induce reduced CBF, as recently reviewed [133]. A recent review concluded that Aβ accumulation only partially explains BBB impairment in AD [56], thus supporting the vascular-mediated neurodegeneration hypothesis.

Detecting neurovascular dysfunction in humans

To date, the majority of evidence of microvascular pathology in AD comes from histological and biofluid analysis. For example, numerous post-mortem histological studies report accumulation of blood-derived proteins (e.g., immunoglobulins, albumin, fibrinogen, and thrombin) in the hippocampus and cortex and/or changes in tight junction endothelial

protein expression at the BBB in human AD brains [76, 81]. Furthermore, a commonly used in vivo measure of BBB breakdown is the albumin ratio (AR), namely the cerebrospinal fluid (CSF) to serum ratio of albumin concentration [22, 75]. Albumin is a relatively large molecule (molecular weight, 67 kDa) that is abundant in blood and cannot cross an intact BBB, thus increased AR is interpreted as an indicator of BBB breakdown. AR is increased in AD patients particularly in those with vascular risk factors [22], as well as in individuals with MCI [115] and cognitively normal apolipoprotein E-ε4 (*APOE4*) carriers [75], which is the major genetic risk factor for sporadic AD. Additional biofluid measures of cerebrovascular dysfunction, including an early increase in CSF pericyte soluble platelet-derived growth factor receptor-β (sPDGFRβ) marker and brain endothelial cells markers, further support a role of vascular changes during early cognitive decline stages, as recently reported in a comprehensive review of NVU cell-specific CSF biomarkers in MCI and AD individuals [166].

Recent advances in neuroimaging approaches are now enabling quantitative, regional detection of cerebrovascular dysfunction in the living human brain. For example, Montagne et al. provide the first in vivo evidence of BBB disruption in the aging hippocampus which worsens in MCI, using a high-resolution MRI method to simultaneously map the blood-to-brain transfer constant of gadolinium (K_{trans}) regionally and quantitatively with a resolution sufficient to image discrete subregions of the hippocampus [115]. Interestingly, they also found that BBB breakdown correlates with increases in CSF levels of the BBB-associated pericyte injury marker sPDGFRβ [115]. Other neuroimaging studies demonstrated CBF dysregulation in mild to moderate AD patients [1] and in older adults at risk for AD prior to detectable Aβ accumulation or brain atrophy [142]. These recent findings support the presence of early vascular changes such as BBB breakdown and abnormal CBF responses in the aging brain that collectively may contribute to accelerated disease progression during preclinical and early stages of AD.

Dynamic and functional neuroimaging of BBB integrity and blood flow

Imaging methodology of BBB permeability

The most widely used technique to investigate the BBB integrity in vivo is dynamic contrast-enhanced (DCE)-MRI with paramagnetic gadolinium-based contrast agents (GBCAs), small molecules (molecular weight, ~1 kDa) that cross disrupted BBB [121]. The transfer rate of GBCAs from the intravascular into the extravascular space of the brain can be measured to determine BBB permeability. Although GBCAs are considered relatively safe compared to iodine-based agents, there are rare reports of nephrogenic systemic [171], and more recently brain retention associated with the linear forms of GBCAs, compared to macrocyclic GBCAs which are at low risk for brain deposition [117].

Several post-processing approaches of DCE dynamic images exist to visualize contrast agent distribution over time. The most straightforward method is to determine the relative signal enhancement in a region-of-interest (ROI), as was used in numerous MRI studies [77, 163, 184, 185]. A stronger signal enhancement of the ROI in the brain extravascular space indicates a higher concentration of contrast agent, which is interpreted as a leakage across the BBB. However, most applications of DCE in the brain have focused on imaging a

relatively high degree of BBB breakdown (such as observed in malignant tumors, multiple sclerosis or stroke), rather than subtle changes in BBB permeability, as found for example during normal aging and MCI stages [115].

The BBB leakage can be determined quantitatively to compute the so-called blood-to-brain transfer constant, K_{trans}. There are several mathematical models available to compute K_{trans} that differ in complexity and assumptions under which they can be applied [158]. For example, a two-compartment models such as the Tofts model [174] assumes that each ROI contains a vascular compartment and an extravascular extracellular space compartment and calculates both the influx and backflux of the tracer, whereas other models such as the Patlak model determines only linear influx of tracer into the brain during the unidirectional entry phase assuming its minimal backflux from brain back into the circulation [129]. Importantly, the K_{trans} values enable detection of a subtly damaged BBB as for example during normal aging and preclinical AD stages and in MCI [115] that is at least one to two orders of magnitude lower than the BBB breakdown found in brain tumors, during relapsing multiple sclerosis attacks, or post-ischemic BBB changes after stroke [103, 156]. Interestingly, Montagne and colleagues showed that the Patlak linear regression model can estimate low vascular permeability (i.e., $K_{trans} = 0.1–0.6 \times 10^{-3}$ min^{-1}) as shown using an optimized DCE-MRI protocol with improved pre- and post-processing analysis [14, 115].

Most pharmacokinetic models require the arterial input function (AIF) to be known. Hence, determination of AIF represents a key issue in the reliable estimation of pharmacokinetic parameters. There are several strategies for AIF selection and the optimal method varies according to pathology, study aims and clinical requirements [28]. In most applications, direct measurement of the AIF is generally considered preferable to population-based AIFs averaged from superior sagittal sinus [104]. Limitations of a population approach are: not always obtainable, susceptible to partial volume and in-flow artifacts, variability in which vessel is sampled, and variability in vessel measurement with approaches ranging from manual ROI selection to methods for automatic vessel detection [33]. Earlier this year, Montagne et al. measured the AIF in each individual from the common carotid artery instead of using an average value from the superior sagittal venous sinus to determine tracer concentration in blood [115]. They have highlighted the fact that individual AIF measurements are important particularly if the studied population diverges by age as changes in blood volume and flow may affect AIF and the final K_{trans} measurements.

The calculation of contrast agent concentration from signal enhancement requires reliable estimation of intrinsic tissue parameters such as the pre-contrast longitudinal relaxation time T1. There are several methods of estimating baseline T1, with variable flip-angle and multiple time repetition being the most common. The effect of uncertainty in T1 estimation on the calculation of contrast agent concentrations has been investigated by Schabel and Parker [144]. They demonstrate that T1 produces a significant concentration bias, which shows the importance of accounting for T1 when assessing BBB disruption in different tissue types [9].

There is also disagreement on whether to describe the capillary bed in terms of blood concentration or plasma concentration by correcting for the hematocrit (Hct). In the latter

case, Hct should ideally be determined for every subject, but a standard value such as Hct = 0.45 is often assumed [158]. In theory, all model equations and resulting parameter values can easily be converted between conventions. Other sources of uncertainty rarely considered in DCE-MRI studies may arise due to a lack of available data. For example, relativity values specific to a contrast agent, field strength and tissue pathology are rarely known, with the consequence that uniform relativity across tissues and compartments is generally assumed. Barnes and coworkers have developed a software (*Rocketship*) suite for dynamic MRI datasets (in particular DCE-MRI) analysis [15]. This software allows for DCE-MRI data analysis using several pharmacokinetic models used currently in the literature as well as data-driven analysis methods. There is a possibility to correct for hematocrit and relativity values specific to the contrast agent used, among many other parameters, which is important for high accuracy of BBB K_{trans} measurements.

Finally, DCE-MRI methodology can still be improved to increase the sensitivity to subtle BBB permeability. Progress can be made by increasing signal-to-noise ratio (SNR) or by increasing spatial resolution. A higher SNR would help to improve the sensitivity to low concentrations of gadolinium due to limited BBB leakage, and a better spatial resolution would help to detect small “hot spots” of leakage. Moving to higher field strengths such as 7 T may help in this regard [178]. Also, a multi-compartment model [129, 174], combined with proper contrast agent concentration calculations [14, 115, 144] and whole-brain voxel-wise analysis methods, should increase sensitivity for low and localized leakage.

Use of BBB imaging in AD

Vascular dysfunction, including BBB breakdown, is increasingly recognized as contributory to AD pathophysiology. In vivo BBB imaging in humans can inform regional brain changes in BBB integrity in the context of physiological circulation and homeostasis, which is advantageous to other common methods to evaluate BBB integrity including analysis of tight junctions and plasma-derived proteins in biofluids or histological markers in post-mortem tissue.

Several early studies using DCE-MRI in the context of AD yielded semi-quantitative BBB analysis interpretations that differ from the current understanding of DCE-MRI. For instance, Wang et al. in 2006 used a DCE-MRI sequence and observed that the signal enhancement curve was higher after contrast agent administration in the hippocampus of MCI compared to control subjects [185]. This was interpreted as lower local blood volume and longer signal retention, indicative of vascular changes in the hippocampus rather than an indication of BBB permeability [185]. Additionally, DCE-MRI analysis in 15 subjects with probable AD and their healthy spouses revealed aberrant temporal patterns of gadolinium-based signal enhancement, interpreted as altered blood–brain–CSF compartment kinetics [163]. Considering the results and timeframe of the study (30 min), the authors concluded that contrast agent accumulation in brain was more conceivable to occur via blood–brain-CSF pathway, rather than blood–CSF–brain pathway [163]. Several groups used DCE-MRI protocols to study BBB integrity in the areas of white matter hyperintensities (WMH) and reported different findings. For instance, BBB permeability in WMH areas was not changed in subjects with dementia [184], but was found to be altered in Binswanger’s disease, a rare,

more diffuse and subcortical form of vascular dementia [77]. These contradictory results may have arisen from methodological differences.

In a more quantitative manner, two recent studies investigated BBB dysfunction in subjects with vascular cognitive impairment [167, 168]. Both studies used a post-contrast scanning time of 24.5 min and the Patlak model to calculate BBB permeability (K_i) maps. The resulting K_i maps were investigated by means of distribution histograms. They demonstrated an increased contrast agent leakage localized in the center of some WMH lesions, though not in every WMH, nor in its periphery, and were inconclusive whether BBB breakdown contributes to WMH lesions or not, suggesting more work needs to be done in this area. Recent study using a novel high-resolution DCE-MRI technique to simultaneously map the K_{trans} constant regionally and quantitatively, and with a resolution sufficient to image discrete regions of the hippocampus [115], suggested that K_{trans} increases linearly with age only in the hippocampus and its CA1 and dentate gyrus regions, which worsens in individuals with MCI as indicated by ~60 % increase in K_{trans} values compared to cognitively intact age-matched controls (Fig. 1). These increases in BBB permeability were not associated with reduced hippocampal volume, suggesting that they may precede the development of tissue damage and hippocampal atrophy [115]. These observations provide the first direct evidence for an age-dependent and regionally selective disruption of the BBB in the hippocampus of cognitively normal individuals, which is exacerbated in MCI.

The above-described studies are heterogeneous in regard to image acquisition and analysis methods, thus care must be taken when comparing results from different studies. For example, tumor studies use higher temporal resolution and shorter imaging duration on average compared with studies of less permeable tissue such as normal appearing brain and dementia [14]. Additionally, motion artifacts can interfere with post-processing DCE datasets even though new motion correction tools have emerged. Due to the wide range of analysis techniques used and their strong dependence on underlying assumptions and acquisition parameters, a lack of inter-study comparability represents a major problem. The importance of appropriate model selection has been demonstrated both theoretically [14, 157] and experimentally in low-permeability brain tissues [42, 103, 115].

Imaging of CBF dysregulation

A full discussion of arterial spin labeling (ASL)-MRI methodology is beyond the scope of this review and has been summarized elsewhere [48]. Briefly, in vivo assessment of CBF via ASL-MRI may be promising as a potential tool for early detection and characterization of AD progression. CBF refers to the rate of delivery of arterial blood to the capillary bed in brain tissue and is typically quantified in milliliters of blood per 100 g of tissue per minute [106]. ASL is a non-invasive and reliable MRI technique [128] that magnetically labels arterial water in the brain and uses it as an endogenous tracer to measure CBF. Because ASL-MRI provides a quantitative measure of CBF in the capillary bed, rather than a relative measure such as the venous blood oxygen level-dependent (BOLD)-functional MRI (fMRI) signal (see later subsection “Blood oxygen level-dependent contribution in functional imaging”), it has the potential to more accurately estimate the magnitude and location of

neuronal function [106], which is an advantage over peripheral measures of vascular pathology.

Use of CBF imaging in AD

Several groups have now reported findings using ASL-MRI in different regions of AD brains. For instance, studies frequently report hypoperfusion to precuneus, posterior cingulate, inferior/superior parietal, and lateral prefrontal cortices [5, 6, 43, 82, 94, 195], though additional areas of reduced perfusion have been described in the temporal lobe including the parahippocampal gyrus and hippocampus [101, 191]. Importantly, as grey matter loss could account for the reduced perfusion signal, several of these studies applied an atrophy correction [4, 43, 94], which did not appear to significantly alter the findings of regional hypoperfusion. In general, these regions displayed greater group level CBF reductions than loss of grey matter tissue, consistent with the notion that the functional change reflected by this measure exceeds volume loss. Interestingly, the above findings correlate with regional reduction of glucose uptake by the brain, as reported in several studies of AD using fluorodeoxyglucose (FDG)-PET imaging [90, 102] (see later subsection “Molecular imaging of AD pathology”). Chen and colleagues directly compared ASL-MRI with FDG-PET acquisition in the same subjects at the same time and found a high correlation between hypoperfusion and impaired glucose uptake by the brain, which is not surprising as glucose uptake is flow dependent [34].

Subjects with MCI are often conceptualized as representing individuals who are transitioning from being cognitively normal to developing symptoms of early AD [131], and some subjects remain in this prodromal stage for several years—up to 7.5 years according to Roe and colleagues [140]—and some revert back to cognitively normal. A limited, but growing, number of studies have applied ASL-MRI to this population [3, 32, 43, 94, 192]. Studies in MCI subjects generally report decreased CBF to precuneus, posterior cingulate, and parietal regions [39, 120], and a further decrease in CBF to hippocampus, caudate, and thalamus in AD compared to no cognitive impairment (NCI) or MCI (Fig. 2a). For example, thalamic CBF decreased 20 % from MCI to AD stages and correlated with subjects’ Dementia Rating Scale (Fig. 2b, c). Interestingly, caudate CBF values also correlated negatively with WML volume, more so in MCI and AD compared to NCI stages (Fig. 2d).

Despite an approximately 40 % global decrease in CBF in AD subjects compared to age-matched cognitively normal adults [10], the medial temporal lobe has been reported to be relatively hyperperfused in at-risk controls (i.e., *APOE4* carriers) and subjects at early stages of AD [4, 43, 61]. For example, in the study by Alsop and colleagues, despite the presence of hypoperfused brain regions, hippocampal and parahippocampal regions were associated with increased CBF in AD subjects relative to age-matched controls [4]. These inconsistent findings remain across studies and are difficult to resolve to date. An appealing reason for this discrepancy has been proposed by Østergaard et al., who suggested that brain capillary dysfunction underlies the development of a neuronal energy crisis which triggers AD [125, 126]. They propose that increased capillary transit time heterogeneity for erythrocytes passing through capillaries decreases the oxygen that can be extracted by the tissue so that, as capillary transit times become more heterogeneous, a higher blood flow is required to

maintain tissue oxygen supply. Obstruction of flow in some capillary branches may therefore trigger an initial compensatory increase in blood flow in order to preserve tissue oxygen extraction and neuronal function. Later on, hypoperfusion (which reflects neurovascular adjustments in an attempt to maintain oxygen availability in the tissue), seen in the progression from normal cognitive aging to mild dementia and AD, is therefore consistent with early disturbances in capillary flow patterns and fits well into established models of AD neuropathology [18]. However, this model needs further testing and validation in human studies.

Despite the clear advantage of ASL-MRI to provide quantitative CBF measurement, several methodological issues currently limit its widespread use. For example, multi-center studies lack ASL-MRI standardization and many of the existing pulse sequences have limitations (e.g., sensitivity to transit time effects, limited brain coverage, low spatial resolution, less sensitivity to white matter CBF) which may account for some of the apparent conflicting data reported in AD, at-risk AD, and MCI stages. The variability in methodology and processing applied across studies has hindered the ability to define standard CBF reference values. Altogether, while ASL-MRI holds promise, it has not been clearly demonstrated to be ready for routine use in clinical trials and clinical practice, remaining a research tool overall. Larger studies in MCI and AD with more direct comparison to existing molecular and neurodegenerative biomarkers will be necessary to determine the clinical value of this approach.

Blood oxygen level-dependent contribution in functional imaging

The BOLD contrast in fMRI has rapidly emerged as a powerful non-invasive technique for studying brain function in humans. The BOLD-fMRI signal is produced by field inhomogeneities induced by deoxyhemoglobin (dHb), an endogenous and natural contrast agent. Specifically, the BOLD-fMRI signal reflects the loss of oxygen from hemoglobin, causing its iron to become paramagnetic, which influences the magnetic field experienced by proton spins within surrounding water molecules [123, 130]. Therefore, changes in the local dHb concentration in the brain lead to modifications in MRI signal intensity [123, 172]. During neuronal activity, an increase of oxygen consumption is instantly followed by a local increase in CBF and CBV, resulting in a net decrease of the amount of dHb, which ultimately alters the MRI signal level [64, 107, 110, 135]. Additionally, it is important to consider the dynamic pattern of the local dHb concentration. Although the dilation of arteries and arterioles can be significant (up to 25 % of baseline) [173], their small volume and high oxygenation means that arteries themselves contribute relatively little to the BOLD-fMRI signal [80]. Veins, however, display large increases in dHb concentration that contribute significantly to the BOLD-fMRI signal. Nevertheless, these increases can be expected to be delayed with respect to the active capillary bed and may even be shifted as a result of the venous drainage system [177]. Despite widespread use for over 20 years, the nature of the BOLD-fMRI signal is a matter of debate [12, 67, 79, 107, 152].

Most fMRI studies treat the BOLD response as an indirect qualitative measure of neuronal activity and interpret BOLD signal differences as changes in neuronal activity. However, the BOLD signal reflects local changes in dHb content, which in turns exhibits an intricate

dependence on changes in CBF, CBV, and the cerebral metabolic rate of oxygen consumption ($CMRO_2$) [27]. $CMRO_2$ is assumed to be most tightly associated with neuronal activity, echoing the notion that neurons necessarily expend energy to accomplish their work [83]. The positive BOLD response observed in most fMRI experiments reflects the fact that CBF increases relatively more than $CMRO_2$, so that local capillary and venous blood are more oxygenated during increased brain activity. Overall, the actual amplitude of the BOLD response is a subtle balance between the relative increases in CBF and $CMRO_2$ [24]. Elements that disturb the connection between CBF and $CMRO_2$, such as aging and degeneration in AD, may therefore alter the BOLD response even when neuronal activity is unchanged. For example, there is growing evidence that variations in the cerebrovascular system due to age and disease can significantly change the BOLD signal and complicate its interpretation. Age-related factors include altered cerebrovascular ultrastructure, reduced blood vessel elasticity, increased atherosclerosis, reduced resting state CBF, decreased resting $CMRO_2$, and reduced vascular reactivity to chemical modulators [47]. In fMRI studies examining the effects of aging, researchers have found a significant age-dependent decrease in the BOLD signal amplitude [26, 170], possibly correlating with age-related decrease in the resistance of the cerebrovascular system [47, 179].

Use of functional MRI in AD

During the past decade, both task-based and resting state BOLD-fMRI studies have proved to be a very useful tool in investigating brain functions and hemodynamic responses in neurodegenerative disorders, especially AD.

In the mid-1990s, activation of the hippocampus and parahippocampal regions during successful memory encoding has been shown in healthy young subjects during various episodic memory tasks using a task-based fMRI paradigm [23, 164, 183]. A few years later, the pioneering task-based fMRI studies on AD also focused on exploring alterations in hippocampal activation [97, 108, 141, 153, 159]. To date, there are several task-dependent fMRI studies which have consistently reported changes in hippocampal activation in AD compared to healthy elderly controls, consistent with impaired memory function [52, 68, 108, 127, 138, 141, 153, 159]. Interestingly, several studies have reported increased prefrontal cortical activity in AD subjects [69, 155, 159], suggesting that other networks may increase activity as an attempted compensatory mechanism during hippocampal failure. Although many of these studies found a decreased hippocampal activity in both MCI and AD subjects, some studies revealed hyperactivity in the hippocampus in MCI individuals [4, 20, 52], which has been interpreted as a compensatory phenomenon, or a harbinger of upcoming hippocampal failure. Cross-sectional studies suggest that this hyperactivity may be present only at early stages of MCI, followed by a loss of activation in late stages of MCI, similar to the pattern seen in individuals with AD [31]. Longitudinal studies furthermore suggest that the presence of hyperactivity at baseline is a predictor of rapid cognitive decline [21, 51, 113], and loss of hippocampal function on serial fMRI [122].

Interestingly, studies of older cognitively normal individuals or middle-aged adults have demonstrated BOLD responses differ by *APOE* genotype [20, 60], including *APOE4* carriers, as well as positive family history of AD [95]. Once more, many task-based fMRI

studies reported a unique impaired functional connectivity/neuronal activity within the hippocampus and to neighboring temporal regions in AD cases. However, modifications in CBF and CBV, as well as changes in $CMRO_2$ level should be accounted for and further discussed since they are known to directly affect the BOLD-fMRI signal and thus may contribute to the observed results. Consistent with this idea, some groups investigated task-dependent BOLD signal changes in preclinical AD and reported that it might reflect altered sensitivity to activation due to changes in baseline blood flow [7, 41].

In addition to task-based fMRI studies, recent functional imaging studies have demonstrated AD-related alterations in the “default mode” network (DMN), during a resting state. The resting state of the human brain was originally identified by its increased activity at wakeful rest, including high resting glucose metabolism and blood flow [74, 136, 151]. An important advantage of resting state fMRI imaging in AD is the ability to scan subjects who are too impaired to actively participate in a task-based scanning paradigm or in whom the interpretation of task-based fMRI responses would be confounded by differences in task performance. The resting state fMRI findings in MCI and AD have been fairly consistent across studies showing abnormalities in the DMN, including the hippocampus, precuneus, medial prefrontal cortex, and lateral parietal cortices. These regions have been reported to be active at rest [71, 136, 169], but during the performance of demanding cognitive tasks, DMN activity decreased dramatically in AD individuals [44, 72, 150, 187].

Overall, a variety of recent reports have explored conditions under which the BOLD-fMRI response is altered or abnormal in AD. While most of these studies interpreted that changed BOLD responses were a reflection of altered underlying neuronal activity, it is becoming increasingly recognized that in some situations, neurovascular coupling itself—including hemodynamic changes of altered blood flow—could be affected. Neurovascular coupling refers to the association of cellular activity and CBF, and alongside the BOLD-fMRI signal, neurovascular coupling is also likely to undergo changes during healthy aging and during AD-related pathological processes. Some of the changes that may occur even in healthy elderly subjects include, for example, increased atherosclerosis [47]. In AD, the presence of Aβ in the cerebral vasculature, together with altered neurotransmitter activity, impairs synaptic, neuronal and glial function [85], may thus lead to an attenuated BOLD response. Furthermore, Dumas and colleagues found changes in the hemodynamic response curve in individuals with cerebral amyloid angiopathy (CAA) which supports that BOLD signal changes are affected by vascular dysregulations present in AD [54]. Additionally, the alterations in BOLD activity reported in AD also appear to be quite regionally specific and dependent on the nature of the cognitive task, thus making it likely that the changes observed in fMRI studies may represent local pathophysiological alterations in neurovascular coupling.

BOLD-fMRI response is variable across subjects. The reproducibility of BOLD signal changes within young healthy individuals during memory encoding tasks across separate days is reported to be reasonable [78, 162]. Some studies have shown moderate-to-excellent test–retest reproducibility of fMRI activation in older and cognitively impaired participants [11, 40, 73, 134, 196]. Longitudinal functional imaging studies are needed to track the evolution of alterations in the fMRI activation pattern over the course of normal aging and

cognitive decline in clinical AD. In addition, fMRI studies should importantly take into account the contribution of structural atrophy observed in dementias. A combination of structural MRI, functional MRI and other imaging techniques such as PET amyloid-imaging may serve as a valuable in vivo method to elucidate AD pathophysiological progression.

One promising area to palliate discrepancies regarding the meaning of the BOLD-fMRI signal is the use of the ASL-MRI technique in combination with BOLD imaging (ASL/BOLD). With the increasing application of fMRI techniques to study AD, there is a growing need for quantitative measures that can more accurately reflect neuronal activity, as well as local hemodynamic changes separately. Therefore, ASL/BOLD imaging would have the potential to distinguish between the BOLD signal and the relative CBF response, and thereby provide a more complete accounting of the functional changes occurring in specified brain regions during the performance of cognitive or other tasks. These combined measures appear promising to characterize the impact of aging, preclinical/clinical AD, genetic risk factors, vascular risk factors, among others, on the CBF response to cognitive functions such as episodic memory. In short, quantitative fMRI with combined ASL/BOLD may address questions that cannot be fully answered with BOLD measures alone [24, 49, 146, 190].

Neuroimaging of vascular pathology and cerebral metabolism

Microbleeding events

Cerebral microbleeds (CMBs) are lesion-based MRI markers visualized as small hypointense regions on T2*- and susceptibility-weighted imaging (SWI-MRI) scans [70]. These punctate lesions are thought to represent hemosiderin-laden macrophages accumulated in perivascular spaces as a result of microhemorrhage [182]. Studies have revealed two patterns of CMB distribution, including subcortical and posterior lobar. Subcortical lesions are thought to be secondary to hypertensive injury, whereas posterior lobar CMBs may be due to CAA [70]. CAA is present in 80–100 % of AD brains, but may also occur in the absence of AD [182]. The posterior lobar involvement of CMBs in CAA is consistent with the general pattern of posterior versus anterior findings from atrophy and WML studies in AD. This evidence supports that evaluating CMBs, in combination with other types of cerebrovascular dysfunction, has the potential to inform the pathophysiological course of AD progression. A full discussion of CMBs in CAA and AD is beyond the scope of this review and is summarized indepth elsewhere [182].

Connectivity and white matter lesions

Diffusion tensor imaging (DTI) is a promising structural MRI modality that has been useful in the study of white matter pathology in AD [2, 29, 139]. This method indexes water diffusion as an indirect measure of microstructural integrity, as discussed in a comprehensive technical review [16]. Specifically, the restriction of water diffusion is anisotropic in brain areas containing large white matter tracts since water is much more likely to diffuse along these tracts than across them. Thus, by tracking the diffusion of water molecules, DTI methods can provide “maps” of white matter tracts in the brain. To the extent that white matter tracts exhibit degenerative changes, the surrounding water molecules can diffuse more freely, making water diffusion considered isotropic. These changes can be quantified

using DTI measures, also called DTI metrics, such as fractional anisotropy (FA) (as depicted in Fig. 3) which indexes the ratio of axial versus radial diffusivity along white matter tracts. Another measure is mean diffusivity (MD), which indexes the overall average of axial and radial diffusivity.

These diffusion maps are statistically analyzed using robust methods, such as tract-based spatial statistics, to evaluate white matter integrity associated with AD. For example, white matter disruptions are observed in MCI compared to control subjects including regions such as the inferior frontal and parahippocampal white matter (Fig. 3). Additionally, DTI studies in AD report widespread and confluent abnormalities in the parietal, temporal, and prefrontal white matter, but posterior white matter changes are most prominent, which are best captured by examining absolute diffusivities [2]. Specifically, the long association fibers and interhemispheric fibers are primarily implicated, including the posterior corpus callosum, cingulum bundle at the level of the posterior cingulate, superior longitudinal fasciculus, fronto-occipital fasciculus, the posterior thalamic radiation, and the superior temporo-parietal white matter [2]. These data are consistent with the posterior to anterior progression model also observed in volumetric grey and white matter studies in AD (see later subsection “Regional brain atrophy”), as are results from a recent study reporting predominantly posterior white matter changes in mild stages and more advanced stages exhibiting both posterior and anterior changes [29].

Less research has been conducted on DTI metrics from grey matter, but the few studies that have been conducted suggest that grey matter microstructural changes may be among the earliest detectible brain changes in AD. In a recent study of individuals with autosomal dominant AD, asymptomatic mutation carriers exhibited increased grey matter MD within the hippocampus, caudate and thalamus before any other structural brain changes were observable [143]. Similarly, other studies of late onset or sporadic AD have also found increased MD within the hippocampus of mildly demented subjects [35, 193]. Although the reason for increased MD within grey matter regions is currently unclear, further study of regional DTI metrics within grey matter may yield new insights into microstructural changes during the earliest stages of AD.

In addition to DTI-metrics and associated white matter tracts, studies utilizing T2/fluid-attenuated inversion recovery (FLAIR)-weighted scans have identified circumscribed areas of hyperintense signal that increase with normal aging [145], but are also associated with AD-related cognitive decline [176]. These WMLs are thought to represent changes in tissue water content secondary to multiple pathological processes, including ischemia, gliosis, and demyelination [145]. These underlying pathological changes may be secondary to cerebral small vessel disease and/or AD-related neurodegeneration. Recent research has focused on differentiating qualitative aspects of WML pathology. These include attempts to parcellate lesions based on the involvement of various neuroanatomical regions or even specific white matter tracts [145]. As with cortical atrophy studies reviewed below (see later subsection “Regional brain atrophy”), more posterior WMLs involving the parietal lobe may be of particular importance in AD, as they correlate more strongly with cognitive impairment and may interact with tau pathology to accelerate clinical progression [176].

Regional brain atrophy

Gross cerebral atrophy is one of the cardinal features of AD neuropathology originally described by Alois Alzheimer in 1906, and structural MRI methodologies therefore became a major focus in studying differences between AD and normal brain aging. Early cerebral atrophy in AD is thought to be due primarily to synaptic loss and subsequently to neuronal loss [148]. The vast majority of early structural neuroimaging studies utilized manual tracing methodologies to quantify the extent of atrophy, but these time-intensive methods limited the study sample size and the number of brain areas that could be assessed. Voxel-based morphometry is an alternative method that does not require manual tracing of a priori ROIs, but may be relatively insensitive to more subtle changes in cortical thickness [50]. The advent of freely available software systems providing semi-automated segmentation and parcellation to assess regional volume and thickness (e.g., *FreeSurfer* software) has improved reproducibility, allowed for larger studies, and provided for a broader survey of brain-wide patterns of cerebral atrophy [58]. Studies comparing older adults with AD to those without dementia report a partly overlapping yet distinct pattern of cerebral cortical atrophy. Specifically, findings indicate the most salient regional atrophy in AD occurs within more posterior regions, including parietal regions such as the precuneus, temporo-parietal cortex and medial-temporal lobes [50, 148] as well as their underlying white matter structures [37].

It is widely recognized that various white matter abnormalities are associated with AD, including Wallerian degeneration, oligodendrocyte loss, and demyelination. Structural neuroimaging studies in MCI and AD reveal that white matter abnormalities are particularly found in the corpus callosum and paraventicular regions. For instance, although prefrontal white matter volume loss occurs as part of normal aging [137], quantification of cerebral white matter atrophy in T1-weighted anatomical images indicate that AD is associated with prominent atrophy of temporal white matter and posterior corpus callosum [105]. In addition to evaluating white matter abnormalities, the majority of volumetric MRI studies in AD have focused on grey matter pathology.

As with normal aging, AD is largely known to be associated with substantial hippocampal atrophy [62, 86]. A recent more sophisticated approach delves beyond overall hippocampal volume to quantify atrophy within specific hippocampal subfields in AD versus normal aging, as reviewed in [62]. Cumulative evidence from structural MRI studies focusing on hippocampal subfields have confirmed that CA1 atrophy is associated with cognitive decline [8], MCI [63], the presence of the *APOE4* allele [98], and progression to AD [8]. However, some studies also indicate additional involvement of other hippocampal subregions [119, 194]. The inconsistent findings of hippocampal subfield morphology in structural MRI analyses are likely due to the great variety of manual tracing methods and/or magnetic field strength-dependent SNR and spatial/temporal resolutions. T1/2-weighted images acquired at 3 and 7 T field strength have different spatial resolution (Fig. 4a) which directly impacts the regional specificity that can be detected, for instance hippocampal analysis in images acquired at 3 Tesla (T) and 7 T can differentially quantify 4 and 7–8 subregions, respectively (Fig. 4b).

Early cognitive decline and AD genetic risk factors are associated with atrophy of hippocampal subfields [8, 62, 63, 98, 119, 119, 194], which is consistent with our recent study in MCI reporting increased BBB K_{trans} permeability predominantly in CA1 and dentate gyrus hippocampal subfields [115]. These data highlight the benefit in adopting a multiparametric approach, for instance combining structural and dynamic MRI sequences, to detect different cerebrovascular measures in parallel. Structural and dynamic modalities could also be used in conjunction with molecular neuroimaging that, through recent advances, now enable in vivo visualization of the magnitude and regional brain distribution of AD-related pathology. Such multiparametric approaches would shed additional light on currently unclear spatial and temporal events in AD pathophysiology, such as the extended prodromal period of AD.

Molecular imaging of AD pathology

Molecular imaging is used to visualize and quantify chemical processes at the cellular and molecular level. The most common form of molecular imaging used to study AD is PET imaging. PET detects pairs of gamma rays emitted from radioactive tracers and is used to produce brain images of tracer binding. PET imaging biomarkers of metabolism and AD neuropathology have substantially enhanced our understanding of AD-specific neural changes in vivo [38, 99]. With the discovery of Aβ-sensitive radioligands over a decade ago, the field experienced a dramatic increase in understanding the neurobiological cascade of events in AD involving pathological burden, neurovascular dysfunction, neurodegeneration, and cognitive decline [86, 99, 116].

The ^{18}F-FDG-PET tracer is a glucose analog that measures glucose transport across the BBB and entry into the brain. Reductions in cerebral metabolic rate of glucose (CMRglc) have been reported in the AD literature for over three decades, consistently demonstrating that individuals with AD have decreased transport of glucose across the BBB and therefore decreased metabolism in AD-affected regions, such as posterior parietal and temporal cortices [13, 55]. Metabolic patterns of FDG-PET uptake have also been shown to discriminate between individuals with normal cognition, MCI, and clinical AD [100, 102]. Measurements derived from FDG-PET do not simply reflect neuronal activity but are impacted by principles of neurovascular coupling involving vascular, astroglial, and neuronal cells, and dynamic CBF [96, 149]. For instance, vasodilation is believed to be a response to neural activity but is impacted by the control of astrocytes on cerebral microcirculation [84, 132]. In vivo and post-mortem studies find that AD and vascular pathology are often comorbid in individuals diagnosed with clinical AD, yet the interactions between amyloid, tau, and vascular pathology in vivo are only beginning to be examined.

Amyloid PET tracers like ^{18}F-AV45 and ^{11}C-PiB (Pittsburgh compound B) have gained traction in multi-site efforts [189] and across large cohorts at single sites [118], and contribute to a growing body of literature of cross-sectional and longitudinal effects of Aβ on the brain [89]. However, the role of Aβ in the pathogenesis of AD is still under debate, and ongoing questions about how Aβ affects brain function and whether amyloid PET is a clinically useful biomarker remain. Many studies have reported associations of Aβ and brain function, brain structure, and cognition. Individuals with significant Aβ have functional

alterations in cortical hubs [25] and connectivity within networks measured with fMRI [161]. Moreover, individuals who are considered amyloid-positive have lower brain volumes and lower cortical thickness in AD-specific regions than amyloid-negative individuals [17]. However, the rate of Aβ accumulation over time may be independent of hippocampal neurodegeneration [87]. There is a debate in the literature whether Aβ accumulation correlates with impaired cognitive function [36], but emerging longitudinal studies suggest that individuals with significant amyloid accumulation are at greater risk for future cognitive decline [180, 181] and have poorer outcomes over time [160, 161]. The relationship between amyloid PET binding and neurovascular integrity in AD are still under investigation, but it is widely viewed that amyloid PET binding occurs not only in neuronal plaques, but vascular plaques as in the case of CAA [30, 92].

Over the last few years, landmark developments of sensitive radioligands that bind to tau, the other hallmark feature of AD, have been reported [88, 124]. These tracers bind to hyperphosphorylated neurofibrillary tangles, the insoluble form of tau, and are not sensitive to tau oligomers. Hyperphosphorylated tau impairs binding to microtubules, thereby reducing neuronal stability, leading to synaptic dysfunction and ultimately cell death [45]. Evidence from animal models suggests a provocative relationship between the accumulation of amyloid and tau for disrupting brain function and cognition in AD. That is, amyloid may accumulate and disrupt neural activity in critical hub regions in the brain [53] while tau may propagate through functional networks in a prion-like manner [65]. The spatial distribution of the pathologies seem distinct, with amyloid depositing first in inferior frontal cortex and spreading to association regions while tau deposition may follow Braak and Braak staging with first sites in limbic regions and then to lateral cortical regions [93]. Data are emerging to show a tight coupling between regional tau PET binding and Braak and Braak staging (reviewed in [45]) and has been validated by post-mortem autoradiography studies [112]. Tau PET is an evolving science that over time will provide answers about the longitudinal sensitivity of diagnostic and prognostic outcomes for AD and other tauopathies. Large-scale efforts that collect multiple markers for metabolism, amyloid, tau, and neurovascular integrity are needed to enhance our understanding of the interaction between events in AD pathophysiology.

Clinical utility

The search for therapies that can modify the course of AD—e.g., to slow, delay, or prevent it—is undoubtedly the most important challenge. That pursuit has led to an exploration for neuroimaging markers to serve as diagnostic tools and/or outcome measures for drug discovery and clinical trials; the clinical utility of each imaging modality will be judged on these fronts. For instance, neuroimaging modalities are already being incorporated into clinical trial design to improve diagnosis (with newly developed dynamic MRI modalities such as DCE- and ASL-MRI) and/or to evaluate the therapeutic efficacy in reducing AD pathophysiology such as vascular (with DCE-MRI) and CBF (with ASL-MRI) dysfunction, atrophy (with structural MRI), disrupted metabolism (with FDG-PET and fMRI), and fibrillary amyloid (with PiB-PET). There is a pronounced clinical need to define dynamic, functional, structural, and molecular phenotypes of AD progression to support AD-specific diagnostic criteria as well as treatment efforts.

Recently improved DCE methodologies yield sensitive regional measures of BBB integrity. DCE images are acquired via a 15-min sequence following GBCA intravenous injection, and are currently used to clinically assess stroke and multiple sclerosis. Thus far, the diagnostic use of DCE has not been applied to AD or other types of dementia; however, recently improved DCE sensitivity has now shown increased hippocampal BBB permeability in CA1 and dentate gyrus subfields of MCI subjects [115]. DCE should therefore be incorporated into clinical practice to evaluate subtle BBB damage that can potentially identify subjects with early AD and related types of dementia. Additionally, recent comparison studies indicate equivalent diagnostic performance between ASL-MRI and PET-MRI methods, but ASL-MRI is advantageous due to its non-invasive, cost-effective, and easily repeatable nature [34]. Hence, ASL-MRI offers promise to clinically detect CBF changes; however, the specificity of ASL-measured CBF to distinguish between AD and other vascular pathologies has not been firmly established, as reduced CBF is also reported in vascular dementia [147] and a post-stroke non-demented group [57], it may mimic changes found in AD. This suggests that regional cerebrovascular measures (i.e., BBB permeability and CBF) should be clinically evaluated in combination with other imaging modalities, biofluid analysis, and clinical information (e.g., neuropsychological performance; vascular/genetic risk factors).

Both task-related and resting state fMRI techniques have the potential to detect early brain dysfunction related to AD; however, thus far the use of fMRI in aging, mild dementia and AD populations has been largely restricted to research studies and clinical trials. Despite the wide use of BOLD-fMRI in research, the BOLD signal remains a matter of debate since it is a direct measure of hemodynamic changes and indirectly reflects neuronal activity. Two current limitations hinder clinical use of fMRI in AD: (1) difficulties related to image acquisition itself, mainly head motion and poor performance due to neurologic deficits; and (2) difficulties related to interpretation in different aging and dementia populations. Resting state fMRI may therefore be more feasible in severely impaired patients.

The clinical application of structural imaging techniques has remained elusive since brain atrophy has a large degree of overlap in both normal and AD-related brain aging [59]. These overlapping distributions become more prominent with advancing age, which thereby attenuates the diagnostic value of brain atrophy scales as patients enter the ninth decade of life [165]. Also, CMBs and WMLs (hyper/hypo-intense signals) and volumetric techniques provide the least information regarding underlying mechanisms or pathology (e.g., gliosis, demyelination, axonal loss). Although it may be possible to detect subtle hippocampal volume changes during early MCI and preclinical phases of AD [19, 154, 175], gross cortical and hippocampal atrophy may not emerge until relatively late in the AD process after observable cognitive decline has occurred [91]. Although DTI metrics offer quantitative indexes of microstructural change, as with other structural imaging modalities, a given change in DTI metrics may reflect a number of different microstructural changes, thus limiting the clinical utility of these scales.

Clinically, many types of AD-related dementias (i.e., fronto-temporal, vascular, mixed, and Lewy-body dementias) in addition to normal aging exhibit both vascular dysfunction and amyloid accumulation. Though amyloid changes occur during preclinical stages of AD, measures of amyloid (PET tracer PiB) and tau (PET tracers targeting tau) do not appear to

be sensitive enough to predict the onset of cognitive impairment and AD clinical diagnosis [140]. Interestingly, many PET-amyloid positive cases will not go on to develop AD or AD-related dementia, suggesting that a concomitant event (perhaps vascular) may be required to initiate cognitive impairment and the neurodegenerative cascade.

Successful treatments of AD and other neurodegenerative diseases lie in early diagnosis and early intervention, as opposed to disease reversal. As our understanding of AD advances, the need for more accurate diagnosis will likely drive neuroimaging towards more ligand- and functional-based technology such that molecular abnormalities and early functional changes can be detected. Multimodal imaging, namely combining information across scanning modalities, is an exciting development that would greatly enhance the clinical utility of each imaging modality and thus potentially improve the sensitivity and/or specificity of neuroimaging to detect various regional subtle cerebrovascular changes related to AD development/progression.

Conclusions

In summary, this review discusses AD-related cerebrovascular dysfunctions measured via different neuroimaging modalities, specifically: BBB integrity (DCE-MRI), CBF dysregulation (ASL-MRI; BOLD fMRI), CBV and $CMRO_2$ (BOLD fMRI), microbleeding events (T2*- and SWI-MRI), white matter connectivity and WML (DTI-MRI), regional brain atrophy (T1- and T2/FLAIR-weighted imaging), CMRglc (FDG-PET), and amyloid deposition (PiB-PET). These neuroimaging approaches are contributing notably to the basic understanding of AD pathophysiology, and have potential diagnostic utility for AD via their ability to detect early neurovascular dysfunction. In particular, new dynamic MRI approaches including DCE- and ASL-type modalities and novel ways of acquiring and of analyzing imaging datasets have freshly contributed strong evidence of vasoreactivity changes and BBB disruption in preclinical AD [39, 115, 120].

The use of newly improved dynamic, functional, structural, and molecular imaging biomarkers conducted simultaneously with molecular biomarker detection in biofluids (i.e., blood and CSF) is necessary to better understand the pathophysiological processes associated with defined stages of AD development. Future longitudinal neuroimaging (i.e., especially DCE- and ASL-MRI) and CSF/blood biomarker studies in human subjects with NCI and/or MCI that also incorporate risk factors for AD (i.e., genetic, vascular, environmental, and lifestyle) should continue to interrogate the role of neurovascular mechanisms in the pathophysiology of dementia due to AD and other causes [116]. Clarifying the precise mechanisms through which vascular insults influence AD development would have enormous benefit in the pursuits to identify novel biological targets for drug development and to aid in patient-directed treatment efforts.

Additional research is necessary to elucidate the temporal sequence of AD pathophysiology (i.e., increased BBB permeability, vasoreactivity disruptions, structural changes and atrophy, functional alterations in brain networks, and molecular changes) and determine the mechanism via which these events and AD risk factors are causally linked to AD etiology. In

conclusion, it is our hope that this issue will enrich the quest to conquer AD using multimodal dynamic, functional, structural, and molecular neuroimaging approaches.

Acknowledgments

We thank the National Institutes of Health (NIH), the Zilkha Senior Scholar program, and the Alzheimer's Association for support. Dr. Zlokovic's research is supported by the NIH through grants R37NS34467, R37AG23084, and R01AG039452. Dr. Pa's research is supported by the NIH through grant R01AG046928 and the Alzheimer's Association grant NIRP12259277. Dr. Toga's research is supported by the NIH through grant P41EB015922. We apologize to those authors whose original work we were not able to cite due to the limited length of this review.

Abbreviations

AD	Alzheimer's disease
AIF	Arterial input function
APOE	Apolipoprotein E
AR	Albumin ratio
ASL	Arterial spin labeling
Aβ	Amyloid beta
BBB	Blood–brain barrier
BOLD	Blood oxygen level-dependent
CA1	Cornu ammonis 1
CAA	Cerebral amyloid angiopathy
CBF	Cerebral blood flow
CBV	Cerebral blood volume
CMB	Cerebral microbleed
CMRglc	Cerebral metabolic rate of glucose
$CMRO_2$	Cerebral metabolic rate of oxygen consumption
CSF	Cerebrospinal fluid
DCE	Dynamic contrast-enhanced
dHb	Deoxyhemoglobin
DMN	Default mode network
DRS	Dementia rating scale
DTI	Diffusion tensor imaging
FA	Fractional anisotropy

FDG	Fluorodeoxyglucose
FLAIR	Fluid-attenuated inversion recovery
fMRI	Functional magnetic resonance imaging
GBCA	Gadolinium-based contrast agent
Hct	Hematocrit
kDa	KiloDalton
MCI	Mild cognitive impairment
MD	Mean diffusivity
MRI	Magnetic resonance imaging
NCI	No cognitive impairment
NVU	Neurovascular unit
PET	Positron emission tomography
PiB	Pittsburgh compound B
ROI	Region-of-interest
SNR	Signal-to-noise ratio
sPDGFRβ	Soluble platelet-derived growth factor receptor-β
SWI	Susceptibility weighted imaging
T	Tesla
WM	White matter
WMH	White matter hyperintensity
WML	White matter lesion

References

1. den Abeelen ASSM, Lagro J, van Beek AHEA, Claassen JAHR. Impaired cerebral autoregulation and vasomotor reactivity in sporadic Alzheimer's disease. Curr Alzheimer Res. 2014; 11:11–17. [PubMed: 24251392]
2. Acosta-Cabronero J, Williams GB, Pengas G, Nestor PJ. Absolute diffusivities define the landscape of white matter degeneration in Alzheimer's disease. Brain J Neurol. 2010; 133:529–539.
3. Alexopoulos P, Sorg C, Förschler A, Grimmer T, Skokou M, Wohlschläger A, Perneczky R, Zimmer C, Kurz A, Preibisch C. Perfusion abnormalities in mild cognitive impairment and mild dementia in Alzheimer's disease measured by pulsed arterial spin labeling MRI. Eur Arch Psychiatry Clin Neurosci. 2012; 262:69–77. [PubMed: 21786091]
4. Alsop DC, Casement M, de Bazelaire C, Fong T, Press DZ. Hippocampal hyperperfusion in Alzheimer's disease. NeuroImage. 2008; 42:1267–1274. [PubMed: 18602481]

5. Alsop DC, Dai W, Grossman M, Detre JA. Arterial spin labeling blood flow MRI: its role in the early characterization of Alzheimer's disease. J Alzheimers Dis JAD. 2010; 20:871–880. [PubMed: 20413865]
6. Alsop DC, Detre JA, Grossman M. Assessment of cerebral blood flow in Alzheimer's disease by spin-labeled magnetic resonance imaging. Ann Neurol. 2000; 47:93–100. [PubMed: 10632106]
7. Alsop DC, Press DZ. Activation and baseline changes in functional MRI studies of Alzheimer disease. Neurology. 2007; 69:1645–1646. [PubMed: 17954778]
8. Apostolova LG, Mosconi L, Thompson PM, Green AE, Hwang KS, Ramirez A, Mistur R, Tsui WH, de Leon MJ. Sub-regional hippocampal atrophy predicts Alzheimer's dementia in the cognitively normal. Neurobiol Aging. 2010; 31:1077–1088. [PubMed: 18814937]
9. Armitage PA, Farrall AJ, Carpenter TK, Doubal FN, Wardlaw JM. Use of dynamic contrast-enhanced MRI to measure subtle blood–brain barrier abnormalities. Magn Reson Imaging. 2011; 29:305–314. [PubMed: 21030178]
10. Asllani I, Habeck C, Scarmeas N, Borogovac A, Brown TR, Stern Y. Multivariate and univariate analysis of continuous arterial spin labeling perfusion MRI in Alzheimer's disease. J Cereb Blood Flow Metab Off J Int Soc Cereb Blood Flow Metab. 2008; 28:725–736.
11. Atri A, O'Brien JL, Sreenivasan A, Rastegar S, Salisbury S, DeLuca AN, O'Keefe KM, LaViolette PS, Rentz DM, Locascio JJ, Sperling RA. Test-retest reliability of memory task functional magnetic resonance imaging in Alzheimer disease clinical trials. Arch Neurol. 2011; 68:599–606. [PubMed: 21555634]
12. Attwell D, Buchan AM, Charpak S, Lauritzen M, Macvicar BA, Newman EA. Glial and neuronal control of brain blood flow. Nature. 2010; 468:232–243. [PubMed: 21068832]
13. Bailly M, Destrieux C, Hommet C, Mondon K, Cottier J-P, Beaufils E, Vierron E, Vercouillie J, Ibazizene M, Voisin T, Payoux P, Barré L, Camus V, Guilloteau D, Ribeiro M-J. Precuneus and cingulate cortex atrophy and hypometabolism in patients with Alzheimer's Disease and mild cognitive impairment: MRI and (18)F-FDG PET quantitative analysis using FreeSurfer. BioMed Res Int. 2015; 2015:583931. [PubMed: 26346648]
14. Barnes SR, Ng TSC, Montagne A, Law M, Zlokovic BV, Jacobs RE. Optimal acquisition and modeling parameters for accurate assessment of low Ktrans blood–brain barrier permeability using dynamic contrast-enhanced MRI. Magn Reson Med. 2015
15. Barnes SR, Ng TSC, Santa-Maria N, Montagne A, Zlokovic BV, Jacobs RE. ROCKETSHIP: a flexible and modular software tool for the planning, processing and analysis of dynamic MRI studies. BMC Med Imaging. 2015; 15:19. [PubMed: 26076957]
16. Basser PJ, Jones DK. Diffusion-tensor MRI: theory, experimental design and data analysis—a technical review. NMR Biomed. 2002; 15:456–467. [PubMed: 12489095]
17. Becker JA, Hedden T, Carmasin J, Maye J, Rentz DM, Putcha D, Fischl B, Greve DN, Marshall GA, Salloway S, Marks D, Buckner RL, Sperling RA, Johnson KA. Amyloid-β associated cortical thinning in clinically normal elderly. Ann Neurol. 2011; 69:1032–1042. [PubMed: 21437929]
18. Bell RD, Winkler EA, Singh I, Sagare AP, Deane R, Wu Z, Holtzman DM, Betsholtz C, Armulik A, Sallstrom J, Berk BC, Zlokovic BV. Apolipoprotein E controls cerebrovascular integrity via cyclophilin A. Nature. 2012; 485:512–516. [PubMed: 22622580]
19. Bernard C, Helmer C, Dilharreguy B, Amieva H, Auriacombe S, Dartigues J-F, Allard M, Catheline G. Time course of brain volume changes in the preclinical phase of Alzheimer's disease. Alzheimers Dement J Alzheimers Assoc. 2014; 10(143–151):e1.
20. Bondi MW, Houston WS, Eyler LT, Brown GG. fMRI evidence of compensatory mechanisms in older adults at genetic risk for Alzheimer disease. Neurology. 2005; 64:501–508. [PubMed: 15699382]
21. Bookheimer SY, Strojwas MH, Cohen MS, Saunders AM, Pericak-Vance MA, Mazziotta JC, Small GW. Patterns of brain activation in people at risk for Alzheimer's disease. N Engl J Med. 2000; 343:450–456. [PubMed: 10944562]
22. Bowman GL, Kaye JA, Quinn JF. Dyslipidemia and blood–brain barrier integrity in Alzheimer's disease. Curr Gerontol Geriatr Res. 2012; 2012:184042. [PubMed: 22654903]

23. Brewer JB, Zhao Z, Desmond JE, Glover GH, Gabrieli JD. Making memories: brain activity that predicts how well visual experience will be remembered. Science. 1998; 281:1185–1187. [PubMed: 9712581]
24. Brown GG, Perthen JE, Liu TT, Buxton RB. A primer on functional magnetic resonance imaging. Neuropsychol Rev. 2007; 17:107–125. [PubMed: 17468956]
25. Buckner RL, Sepulcre J, Talukdar T, Krienen FM, Liu H, Hedden T, Andrews-Hanna JR, Sperling RA, Johnson KA. Cortical hubs revealed by intrinsic functional connectivity: mapping, assessment of stability, and relation to Alzheimer's disease. J Neurosci Off J Soc Neurosci. 2009; 29:1860–1873.
26. Buckner RL, Snyder AZ, Sanders AL, Raichle ME, Morris JC. Functional brain imaging of young, nondemented, and demented older adults. J Cogn Neurosci. 2000; 12(Suppl 2):24–34. [PubMed: 11506645]
27. Buxton RB, Uludağ K, Dubowitz DJ, Liu TT. Modeling the hemodynamic response to brain activation. NeuroImage. 2004; 23(Suppl 1):S220–S233. [PubMed: 15501093]
28. Calamante F. Arterial input function in perfusion MRI: a comprehensive review. Prog Nucl Magn Reson Spectrosc. 2013; 74:1–32. [PubMed: 24083460]
29. Canu E, Agosta F, Spinelli EG, Magnani G, Marcone A, Scola E, Falautano M, Comi G, Falini A, Filippi M. White matter microstructural damage in Alzheimer's disease at different ages of onset. Neurobiol Aging. 2013; 34:2331–2340. [PubMed: 23623599]
30. Catafau AM, Bullich S. Amyloid PET imaging: applications beyond Alzheimer's disease. Clin Transl Imaging. 2015; 3:39–55. [PubMed: 25741489]
31. Celone KA, Calhoun VD, Dickerson BC, Atri A, Chua EF, Miller SL, DePeau K, Rentz DM, Selkoe DJ, Blacker D, Albert MS, Sperling RA. Alterations in memory networks in mild cognitive impairment and Alzheimer's disease: an independent component analysis. J Neurosci Off J Soc Neurosci. 2006; 26:10222–10231.
32. Chao LL, Pa J, Duarte A, Schuff N, Weiner MW, Kramer JH, Miller BL, Freeman KM, Johnson JK. Patterns of cerebral hypoperfusion in amnestic and dysexecutive MCI. Alzheimer Dis Assoc Disord. 2009; 23:245–252. [PubMed: 19812467]
33. Chen J, Yao J, Thomasson D. Automatic determination of arterial input function for dynamic contrast enhanced MRI in tumor assessment. Med Image Comput Comput-Assist Interv MICCAI Int Conf Med Image Comput Comput-Assist Interv. 2008; 11:594–601.
34. Chen Y, Wolk DA, Reddin JS, Korczykowski M, Martinez PM, Musiek ES, Newberg AB, Julin P, Arnold SE, Greenberg JH, Detre JA. Voxel-level comparison of arterial spin-labeled perfusion MRI and FDG-PET in Alzheimer disease. Neurology. 2011; 77:1977–1985. [PubMed: 22094481]
35. Cherubini A, Péran P, Spoletini I, Di Paola M, Di Iulio F, Hagberg GE, Sancesario G, Gianni W, Bossù P, Caltagirone C, Sabatini U, Spalletta G. Combined volumetry and DTI in subcortical structures of mild cognitive impairment and Alzheimer's disease patients. J Alzheimers Dis JAD. 2010; 19:1273–1282. [PubMed: 20308792]
36. Chételat G, Villemagne VL, Pike KE, Ellis KA, Bourgeat P, Jones G, O'Keefe GJ, Salvado O, Szoeke C, Martins RN, Ames D, Masters CL, Rowe CC. Australian Imaging Biomarkers and Lifestyle Study of ageing (AIBL) Research Group. Independent contribution of temporal beta-amyloid deposition to memory decline in the pre-dementia phase of Alzheimer's disease. Brain J Neurol. 2011; 134:798–807.
37. Choo IH, Lee DY, Oh JS, Lee JS, Lee DS, Song IC, Youn JC, Kim SG, Kim KW, Jhoo JH, Woo JI. Posterior cingulate cortex atrophy and regional cingulum disruption in mild cognitive impairment and Alzheimer's disease. Neurobiol Aging. 2010; 31:772–779. [PubMed: 18687503]
38. Clark CM, Schneider JA, Bedell BJ, Beach TG, Bilker WB, Mintun MA, Pontecorvo MJ, Hefti F, Carpenter AP, Flitter ML, Krautkramer MJ, Kung HF, Coleman RE, Doraiswamy PM, Fleisher AS, Sabbagh MN, Sadowsky CH, Reiman EP, Reiman PEM, Zehntner SP, Skovronsky DM. AV45-A07 Study Group. Use of florbetapir-PET for imaging beta-amyloid pathology. JAMA. 2011; 305:275–283. [PubMed: 21245183]
39. Clark LR, Nation DA, Wierenga CE, Bangen KJ, Dev SI, Shin DD, Delano-Wood L, Liu TT, Rissman RA, Bondi MW. Elevated cerebrovascular resistance index is associated with cognitive dysfunction in the very-old. Alzheimers Res Ther. 2015; 7:3. [PubMed: 27391477]

40. Clément F, Belleville S. Test-retest reliability of fMRI verbal episodic memory paradigms in healthy older adults and in persons with mild cognitive impairment. Hum Brain Mapp. 2009; 30:4033–4047. [PubMed: 19492301]
41. Cohen ER, Ugurbil K, Kim S-G. Effect of basal conditions on the magnitude and dynamics of the blood oxygenation level-dependent fMRI response. J Cereb Blood Flow Metab Off J Int Soc Cereb Blood Flow Metab. 2002; 22:1042–1053.
42. Cramer SP, Larsson HBW. Accurate determination of blood–brain barrier permeability using dynamic contrast-enhanced T1-weighted MRI: a simulation and in vivo study on healthy subjects and multiple sclerosis patients. J Cereb Blood Flow Metab Off J Int Soc Cereb Blood Flow Metab. 2014; 34:1655–1665.
43. Dai W, Lopez OL, Carmichael OT, Becker JT, Kuller LH, Gach HM. Mild cognitive impairment and alzheimer disease: patterns of altered cerebral blood flow at MR imaging. Radiology. 2009; 250:856–866. [PubMed: 19164119]
44. Damoiseaux JS, Beckmann CF, Arigita EJS, Barkhof F, Scheltens P, Stam CJ, Smith SM, Rombouts SARB. Reduced resting-state brain activity in the “default network” in normal aging. Cereb Cortex N Y N 1991. 2008; 18:1856–1864.
45. Dani M, Brooks DJ, Edison P. Tau imaging in neurodegenerative diseases. Eur J Nucl Med Mol Imaging. 2015
46. Deane R, Wu Z, Zlokovic BV. RAGE (yin) versus LRP (yang) balance regulates alzheimer amyloid beta-peptide clearance through transport across the blood–brain barrier. Stroke J Cereb Circ. 2004; 35:2628–2631.
47. D’Esposito M, Deouell LY, Gazzaley A. Alterations in the BOLD fMRI signal with ageing and disease: a challenge for neuroimaging. Nat Rev Neurosci. 2003; 4:863–872. [PubMed: 14595398]
48. Detre JA, Rao H, Wang DJJ, Chen YF, Wang Z. Applications of arterial spin labeled MRI in the brain. J Magn Reson Imaging JMRI. 2012; 35:1026–1037. [PubMed: 22246782]
49. Detre JA, Wang J. Technical aspects and utility of fMRI using BOLD and ASL. Clin Neurophysiol Off J Int Fed Clin Neurophysiol. 2002; 113:621–634.
50. Diaz-de-Grenu LZ, Acosta-Cabronero J, Chong YFV, Pereira JMS, Sajjadi SA, Williams GB, Nestor PJ. A brief history of voxel-based grey matter analysis in Alzheimer’s disease. J Alzheimers Dis JAD. 2014; 38:647–659. [PubMed: 24037033]
51. Dickerson BC, Salat DH, Bates JF, Atiya M, Killiany RJ, Greve DN, Dale AM, Stern CE, Blacker D, Albert MS, Sperling RA. Medial temporal lobe function and structure in mild cognitive impairment. Ann Neurol. 2004; 56:27–35. [PubMed: 15236399]
52. Dickerson BC, Salat DH, Greve DN, Chua EF, Rand-Giovannetti E, Rentz DM, Bertram L, Mullin K, Tanzi RE, Blacker D, Albert MS, Sperling RA. Increased hippocampal activation in mild cognitive impairment compared to normal aging and AD. Neurology. 2005; 65:404–411. [PubMed: 16087905]
53. Drzezga A, Becker JA, Van Dijk KRA, Sreenivasan A, Talukdar T, Sullivan C, Schultz AP, Sepulcre J, Putcha D, Greve D, Johnson KA, Sperling RA. Neuronal dysfunction and disconnection of cortical hubs in non-demented subjects with elevated amyloid burden. Brain J Neurol. 2011; 134:1635–1646.
54. Dumas A, Dierksen GA, Gurol ME, Halpin A, Martinez-Ramirez S, Schwab K, Rosand J, Viswanathan A, Salat DH, Polimeni JR, Greenberg SM. Functional magnetic resonance imaging detection of vascular reactivity in cerebral amyloid angiopathy. Ann Neurol. 2012; 72:76–81. [PubMed: 22829269]
55. Edison P, Archer HA, Hinz R, Hammers A, Pavese N, Tai YF, Hotton G, Cutler D, Fox N, Kennedy A, Rossor M, Brooks DJ. Amyloid, hypometabolism, and cognition in Alzheimer disease: an [11C]PIB and [18F]FDG PET study. Neurology. 2007; 68:501–508. [PubMed: 17065593]
56. Erickson MA, Banks WA. Blood–brain barrier dysfunction as a cause and consequence of Alzheimer’s disease. J Cereb Blood Flow Metab Off J Int Soc Cereb Blood Flow Metab. 2013; 33:1500–1513.

57. Firbank MJ, He J, Blamire AM, Singh B, Danson P, Kalaria RN, O'Brien JT. Cerebral blood flow by arterial spin labeling in poststroke dementia. Neurology. 2011; 76:1478–1484. [PubMed: 21518997]
58. Fischl B, Salat DH, Busa E, Albert M, Dieterich M, Haselgrove C, van der Kouwe A, Killiany R, Kennedy D, Klaveness S, Montillo A, Makris N, Rosen B, Dale AM. Whole brain segmentation: automated labeling of neuroanatomical structures in the human brain. Neuron. 2002; 33:341–355. [PubMed: 11832223]
59. Fjell AM, McEvoy L, Holland D, Dale AM, Walhovd KB. Alzheimer's Disease Neuroimaging Initiative. Brain changes in older adults at very low risk for Alzheimer's disease. J Neurosci Off J Soc Neurosci. 2013; 33:8237–8242.
60. Fleisher AS, Houston WS, Eyler LT, Frye S, Jenkins C, Thal LJ, Bondi MW. Identification of Alzheimer disease risk by functional magnetic resonance imaging. Arch Neurol. 2005; 62:1881–1888. [PubMed: 16344346]
61. Fleisher AS, Podraza KM, Bangen KJ, Taylor C, Sherzai A, Sidhar K, Liu TT, Dale AM, Buxton RB. Cerebral perfusion and oxygenation differences in Alzheimer's disease risk. Neurobiol Aging. 2009; 30:1737–1748. [PubMed: 18325636]
62. de Flores R, La Joie R, Chételat G. Structural imaging of hippocampal subfields in healthy aging and Alzheimer's disease. Neuroscience. 2015; 309:29–50. [PubMed: 26306871]
63. de Flores R, La Joie R, Landeau B, Perrotin A, Mézenge F, de La Sayette V, Eustache F, Desgranges B, Chételat G. Effects of age and Alzheimer's disease on hippocampal subfields: comparison between manual and FreeSurfer volumetry. Hum Brain Mapp. 2015; 36:463–474. [PubMed: 25231681]
64. Fox PT, Raichle ME. Focal physiological uncoupling of cerebral blood flow and oxidative metabolism during somatosensory stimulation in human subjects. Proc Natl Acad Sci USA. 1986; 83:1140–1144. [PubMed: 3485282]
65. Frost B, Jacks RL, Diamond MI. Propagation of tau misfolding from the outside to the inside of a cell. J Biol Chem. 2009; 284:12845–12852. [PubMed: 19282288]
66. Ganguli M, Dodge HH, Shen C, DeKosky ST. Mild cognitive impairment, amnestic type: an epidemiologic study. Neurology. 2004; 63:115–121. [PubMed: 15249620]
67. Girouard H, Iadecola C. Neurovascular coupling in the normal brain and in hypertension, stroke, and Alzheimer disease. J Appl Physiol Bethesda Md 1985. 2006; 100:328–335.
68. Golby A, Silverberg G, Race E, Gabrieli S, O'Shea J, Knierim K, Stebbins G, Gabrieli J. Memory encoding in Alzheimer's disease: an fMRI study of explicit and implicit memory. Brain J Neurol. 2005; 128:773–787.
69. Grady CL, McIntosh AR, Beig S, Keightley ML, Burian H, Black SE. Evidence from functional neuroimaging of a compensatory prefrontal network in Alzheimer's disease. J Neurosci Off J Soc Neurosci. 2003; 23:986–993.
70. Greenberg SM, Vernooij MW, Cordonnier C, Viswanathan A, Al-Shahi Salman R, Warach S, Launer LJ, Van Buchem MA, Breteler MM. Microbleed Study Group. Cerebral microbleeds: a guide to detection and interpretation. Lancet Neurol. 2009; 8:165–174. [PubMed: 19161908]
71. Greicius MD, Krasnow B, Reiss AL, Menon V. Functional connectivity in the resting brain: a network analysis of the default mode hypothesis. Proc Natl Acad Sci USA. 2003; 100:253–258. [PubMed: 12506194]
72. Greicius MD, Srivastava G, Reiss AL, Menon V. Default-mode network activity distinguishes Alzheimer's disease from healthy aging: evidence from functional MRI. Proc Natl Acad Sci USA. 2004; 101:4637–4642. [PubMed: 15070770]
73. Guo CC, Kurth F, Zhou J, Mayer EA, Eickhoff SB, Kramer JH, Seeley WW. One-year test–retest reliability of intrinsic connectivity network fMRI in older adults. NeuroImage. 2012; 61:1471–1483. [PubMed: 22446491]
74. Gusnard DA, Raichle ME, Raichle ME. Searching for a baseline: functional imaging and the resting human brain. Nat Rev Neurosci. 2001; 2:685–694. [PubMed: 11584306]
75. Halliday MR, Pomara N, Sagare AP, Mack WJ, Frangione B, Zlokovic BV. Relationship between cyclophilin a levels and matrix metalloproteinase 9 activity in cerebrospinal fluid of cognitively

normal apolipoprotein e4 carriers and blood–brain barrier breakdown. JAMA Neurol. 2013; 70:1198–1200. [PubMed: 24030206]

76. Halliday MR, Rege SV, Ma Q, Zhao Z, Miller CA, Winkler EA, Zlokovic BV. Accelerated pericyte degeneration and blood–brain barrier breakdown in apolipoprotein E4 carriers with Alzheimer's disease. J Cereb Blood Flow Metab Off J Int Soc Cereb Blood Flow Metab. 2015
77. Hanyu H, Asano T, Tanaka Y, Iwamoto T, Takasaki M, Abe K. Increased blood–brain barrier permeability in white matter lesions of Binswanger's disease evaluated by contrast-enhanced MRI. Dement Geriatr Cogn Disord. 2002; 14:1–6. [PubMed: 12053125]
78. Harrington GS, Tomaszewski Farias S, Buonocore MH, Yonelinas AP. The intersubject and intrasubject reproducibility of FMRI activation during three encoding tasks: implications for clinical applications. Neuroradiology. 2006; 48:495–505. [PubMed: 16703360]
79. Hillman EMC. Coupling mechanism and significance of the BOLD signal: a status report. Annu Rev Neurosci. 2014; 37:161–181. [PubMed: 25032494]
80. Hillman EMC, Devor A, Bouchard MB, Dunn AK, Krauss GW, Skoch J, Bacskai BJ, Dale AM, Boas DA. Depth-resolved optical imaging and microscopy of vascular compartment dynamics during somatosensory stimulation. NeuroImage. 2007; 35:89–104. [PubMed: 17222567]
81. Hultman K, Strickland S, Norris EH. The APOE ε4/ε4 genotype potentiates vascular fibrin(ogen) deposition in amyloid-laden vessels in the brains of Alzheimer's disease patients. J Cereb Blood Flow Metab Off J Int Soc Cereb Blood Flow Metab. 2013; 33:1251–1258.
82. Hu WT, Wang Z, Lee VM-Y, Trojanowski JQ, Detre JA, Grossman M. Distinct cerebral perfusion patterns in FTLD and AD. Neurology. 2010; 75:881–888. [PubMed: 20819999]
83. Hyder F. Neuroimaging with calibrated FMRI. Stroke J Cereb Circ. 2004; 35:2635–2641.
84. Iadecola C. Regulation of the cerebral microcirculation during neural activity: is nitric oxide the missing link? Trends Neurosci. 1993; 16:206–214. [PubMed: 7688160]
85. Iadecola C. Cerebrovascular effects of amyloid-beta peptides: mechanisms and implications for Alzheimer's dementia. Cell Mol Neurobiol. 2003; 23:681–689. [PubMed: 14514024]
86. Jack CR, Knopman DS, Jagust WJ, Petersen RC, Weiner MW, Aisen PS, Shaw LM, Vemuri P, Wiste HJ, Weigand SD, Lesnick TG, Pankratz VS, Donohue MC, Trojanowski JQ. Tracking pathophysiological processes in Alzheimer's disease: an updated hypothetical model of dynamic biomarkers. Lancet Neurol. 2013; 12:207–216. [PubMed: 23332364]
87. Jack CR, Wiste HJ, Knopman DS, Vemuri P, Mielke MM, Weigand SD, Senjem ML, Gunter JL, Lowe V, Gregg BE, Pankratz VS, Petersen RC. Rates of β-amyloid accumulation are independent of hippocampal neurodegeneration. Neurology. 2014; 82:1605–1612. [PubMed: 24706010]
88. Jagust W. Time for tau. Brain J Neurol. 2014; 137:1570–1571.
89. Jagust W. Is amyloid-β harmful to the brain? Insights from human imaging studies. Brain J Neurol. 2015
90. Jagust WJ, Bandy D, Chen K, Foster NL, Landau SM, Mathis CA, Price JC, Reiman EM, Skovronsky D, Koeppe RA. Alzheimer's Disease Neuroimaging Initiative. The Alzheimer's Disease Neuroimaging Initiative positron emission tomography core. Alzheimers Dement J Alzheimers Assoc. 2010; 6:221–229.
91. Jedynak BM, Lang A, Liu B, Katz E, Zhang Y, Wyman BT, Raunig D, Jedynak CP, Caffo B, Prince JL. Alzheimer's Disease Neuroimaging Initiative. A computational neurodegenerative disease progression score: method and results with the Alzheimer's disease Neuroimaging Initiative cohort. NeuroImage. 2012; 63:1478–1486. [PubMed: 22885136]
92. Johnson KA, Gregas M, Becker JA, Kinnecom C, Salat DH, Moran EK, Smith EE, Rosand J, Rentz DM, Klunk WE, Mathis CA, Price JC, Dekosky ST, Fischman AJ, Greenberg SM. Imaging of amyloid burden and distribution in cerebral amyloid angiopathy. Ann Neurol. 2007; 62:229–234. [PubMed: 17683091]
93. Johnson KA, Schultz A, Betensky RA, Becker JA, Sepulcre J, Rentz D, Mormino E, Chhatwal J, Amariglio R, Papp K, Marshall G, Albers M, Mauro S, Pepin L, Alverio J, Judge K, Philiossaint M, Shoup T, Yokell D, Dickerson B, Gomez-Isla T, Hyman B, Vasdev N, Sperling R. Tau PET imaging in aging and early Alzheimer's disease. Ann Neurol. 2015
94. Johnson NA, Jahng G-H, Weiner MW, Miller BL, Chui HC, Jagust WJ, Gorno-Tempini ML, Schuff N. Pattern of cerebral hypoperfusion in Alzheimer disease and mild cognitive impairment

measured with arterial spin-labeling MR imaging: initial experience. Radiology. 2005; 234:851–859. [PubMed: 15734937]

95. Johnson SC, Schmitz TW, Trivedi MA, Ries ML, Torgerson BM, Carlsson CM, Asthana S, Hermann BP, Sager MA. The influence of Alzheimer disease family history and apolipoprotein E epsilon4 on mesial temporal lobe activation. J Neurosci Off J Soc Neurosci. 2006; 26:6069–6076.
96. Kasischke KA, Vishwasrao HD, Fisher PJ, Zipfel WR, Webb WW. Neural activity triggers neuronal oxidative metabolism followed by astrocytic glycolysis. Science. 2004; 305:99–103. [PubMed: 15232110]
97. Kato T, Knopman D, Liu H. Dissociation of regional activation in mild AD during visual encoding: a functional MRI study. Neurology. 2001; 57:812–816. [PubMed: 11552009]
98. Kerchner GA, Berdnik D, Shen JC, Bernstein JD, Fenesy MC, Deutsch GK, Wyss-Coray T, Rutt BK. APOE ε4 worsens hippocampal CA1 apical neuropil atrophy and episodic memory. Neurology. 2014; 82:691–697. [PubMed: 24453080]
99. Klunk WE, Engler H, Nordberg A, Wang Y, Blomqvist G, Holt DP, Bergström M, Savitcheva I, Huang G, Estrada S, Ausén B, Debnath ML, Barletta J, Price JC, Sandell J, Lopresti BJ, Wall A, Koivisto P, Antoni G, Mathis CA, Långström B. Imaging brain amyloid in Alzheimer's disease with Pittsburgh Compound-B. Ann Neurol. 2004; 55:306–319. [PubMed: 14991808]
100. Knopman DS. Diagnostic tests for Alzheimer disease: FDG-PET imaging is a player in search of a role. Neurol Clin Pract. 2012; 2:151–153. [PubMed: 23634363]
101. Lacalle-Aurioles M, Mateos-Pérez JM, Guzmán-De-Villoria JA, Olazarán J, Cruz-Orduña I, Alemán-Gómez Y, Martino M-E, Desco M. Cerebral blood flow is an earlier indicator of perfusion abnormalities than cerebral blood volume in Alzheimer's disease. J Cereb Blood Flow Metab Off J Int Soc Cereb Blood Flow Metab. 2014; 34:654–659.
102. Landau SM, Harvey D, Madison CM, Koeppe RA, Reiman EM, Foster NL, Weiner MW, Jagust WJ. Alzheimer's Disease Neuroimaging Initiative. Associations between cognitive, functional, and FDG-PET measures of decline in AD and MCI. Neurobiol Aging. 2011; 32:1207–1218. [PubMed: 19660834]
103. Larsson HBW, Courivaud F, Rostrup E, Hansen AE. Measurement of brain perfusion, blood volume, and blood–brain barrier permeability, using dynamic contrast-enhanced T(1)-weighted MRI at 3 tesla. Magn Reson Med. 2009; 62:1270–1281. [PubMed: 19780145]
104. Lavini C, Verhoeff JJC. Reproducibility of the gadolinium concentration measurements and of the fitting parameters of the vascular input function in the superior sagittal sinus in a patient population. Magn Reson Imaging. 2010; 28:1420–1430. [PubMed: 20817379]
105. Li J, Pan P, Huang R, Shang H. A meta-analysis of voxel-based morphometry studies of white matter volume alterations in Alzheimer's disease. Neurosci Biobehav Rev. 2012; 36:757–763. [PubMed: 22192882]
106. Liu TT, Brown GG. Measurement of cerebral perfusion with arterial spin labeling: Part 1. Methods. J Int Neuropsychol Soc JINS. 2007; 13:517–525. [PubMed: 17445301]
107. Logothetis NK. Neurovascular uncoupling: much ado about nothing. Front Neuroenergetics. 2010
108. Machulda MM, Ward HA, Borowski B, Gunter JL, Cha RH, O'Brien PC, Petersen RC, Boeve BF, Knopman D, Tang-Wai DF, Ivnik RJ, Smith GE, Tangalos EG, Jack CR. Comparison of memory fMRI response among normal, MCI, and Alzheimer's patients. Neurology. 2003; 61:500–506. [PubMed: 12939424]
109. Mackic JB, Bading J, Ghiso J, Walker L, Wisniewski T, Frangione B, Zlokovic BV. Circulating amyloid-beta peptide crosses the blood–brain barrier in aged monkeys and contributes to Alzheimer's disease lesions. Vascul Pharmacol. 2002; 38:303–313. [PubMed: 12529925]
110. Malonek D, Dirnagl U, Lindauer U, Yamada K, Kanno I, Grinvald A. Vascular imprints of neuronal activity: relationships between the dynamics of cortical blood flow, oxygenation, and volume changes following sensory stimulation. Proc Natl Acad Sci USA. 1997; 94:14826–14831. [PubMed: 9405698]
111. Mann GE, Zlokovic BV, Yudilevich DL. Evidence for a lactate transport system in the sarcolemmal membrane of the perfused rabbit heart: kinetics of unidirectional influx, carrier specificity and effects of glucagon. Biochim Biophys Acta. 1985; 819:241–248. [PubMed: 4041458]

112. Marquié M, Normandin MD, Vanderburg CR, Costantino IM, Bien EA, Rycyna LG, Klunk WE, Mathis CA, Ikonomovic MD, Debnath ML, Vasdev N, Dickerson BC, Gomperts SN, Growdon JH, Johnson KA, Frosch MP, Hyman BT, Gómez-Isla T. Validating novel tau positron emission tomography tracer [F-18]-AV-1451 (T807) on postmortem brain tissue. Ann Neurol. 2015; 78:787–800. [PubMed: 26344059]
113. Miller SL, Fenstermacher E, Bates J, Blacker D, Sperling RA, Dickerson BC. Hippocampal activation in adults with mild cognitive impairment predicts subsequent cognitive decline. J Neurol Neurosurg Psychiatry. 2008; 79:630–635. [PubMed: 17846109]
114. Mitchell AJ, Shiri-Feshki M. Rate of progression of mild cognitive impairment to dementia–meta-analysis of 41 robust inception cohort studies. Acta Psychiatr Scand. 2009; 119:252–265. [PubMed: 19236314]
115. Montagne A, Barnes SR, Sweeney MD, Halliday MR, Sagare AP, Zhao Z, Toga AW, Jacobs RE, Liu CY, Amezcua L, Harrington MG, Chui HC, Law M, Zlokovic BV. Blood–brain barrier breakdown in the aging human hippocampus. Neuron. 2015; 85:296–302. [PubMed: 25611508]
116. Montagne A, Pa J, Zlokovic BV. Vascular plasticity and cognition during normal aging and dementia. JAMA Neurol. 2015; 72:495–496. [PubMed: 25751405]
117. Montagne A, Toga AW, Zlokovic BV. Blood–brain barrier permeability and gadolinium: benefits and potential pitfalls in research. JAMA Neurol. 2015
118. Mormino EC, Betensky RA, Hedden T, Schultz AP, Ward A, Huijbers W, Rentz DM, Johnson KA, Sperling RA. Alzheimer's Disease Neuroimaging Initiative, Australian Imaging Biomarkers and Lifestyle Flagship Study of Ageing, Harvard Aging Brain Study. Amyloid and APOE ε4 interact to influence short-term decline in preclinical Alzheimer disease. Neurology. 2014; 82:1760–1767. [PubMed: 24748674]
119. Mueller SG, Schuff N, Raptentsetsang S, Elman J, Weiner MW. Selective effect of Apo e4 on CA3 and dentate in normal aging and Alzheimer's disease using high resolution MRI at 4 T. NeuroImage. 2008; 42:42–48. [PubMed: 18534867]
120. Nation DA, Wierenga CE, Clark LR, Dev SI, Stricker NH, Jak AJ, Salmon DP, Delano-Wood L, Bangen KJ, Rissman RA, Liu TT, Bondi MW. Cortical and subcortical cerebrovascular resistance index in mild cognitive impairment and Alzheimer's disease. J Alzheimers Dis JAD. 2013; 36:689–698. [PubMed: 23666173]
121. Nitta T, Hata M, Gotoh S, Seo Y, Sasaki H, Hashimoto N, Furuse M, Tsukita S. Size-selective loosening of the blood–brain barrier in claudin-5-deficient mice. J Cell Biol. 2003; 161:653–660. [PubMed: 12743111]
122. O'Brien JL, O'Keefe KM, LaViolette PS, DeLuca AN, Blacker D, Dickerson BC, Sperling RA. Longitudinal fMRI in elderly reveals loss of hippocampal activation with clinical decline. Neurology. 2010; 74:1969–1976. [PubMed: 20463288]
123. Ogawa S, Lee TM, Kay AR, Tank DW. Brain magnetic resonance imaging with contrast dependent on blood oxygenation. Proc Natl Acad Sci USA. 1990; 87:9868–9872. [PubMed: 2124706]
124. Okamura N, Harada R, Furumoto S, Arai H, Yanai K, Kudo Y. Tau PET imaging in Alzheimer's disease. Curr Neurol Neurosci Rep. 2014; 14:500. [PubMed: 25239654]
125. Østergaard L, Aamand R, Gutiérrez-Jiménez E, Ho Y-CL, Blicher JU, Madsen SM, Nagenthiraja K, Dalby RB, Drasbek KR, Møller A, Brændgaard H, Mouridsen K, Jespersen SN, Jensen MS, West MJ. The capillary dysfunction hypothesis of Alzheimer's disease. Neurobiol Aging. 2013; 34:1018–1031. [PubMed: 23084084]
126. Østergaard L, Jespersen SN, Engedahl T, Gutiérrez Jiménez E, Ashkanian M, Hansen MB, Eskildsen S, Mouridsen K. Capillary dysfunction: its detection and causative role in dementias and stroke. Curr Neurol Neurosci Rep. 2015; 15:37. [PubMed: 25956993]
127. Pariente J, Cole S, Henson R, Clare L, Kennedy A, Rossor M, Cipoloti L, Puel M, Demonet JF, Chollet F, Frackowiak RSJ. Alzheimer's patients engage an alternative network during a memory task. Ann Neurol. 2005; 58:870–879. [PubMed: 16315273]
128. Parkes LM, Rashid W, Chard DT, Tofts PS. Normal cerebral perfusion measurements using arterial spin labeling: reproducibility, stability, and age and gender effects. Magn Reson Med. 2004; 51:736–743. [PubMed: 15065246]

129. Patlak CS, Blasberg RG, Fenstermacher JD. Graphical evaluation of blood-to-brain transfer constants from multiple-time uptake data. J Cereb Blood Flow Metab Off J Int Soc Cereb Blood Flow Metab. 1983; 3:1–7.
130. Pauling L, Coryell CD. The magnetic properties and structure of hemoglobin, oxyhemoglobin and carbonmonoxyhemoglobin. Proc Natl Acad Sci USA. 1936; 22:210–216. [PubMed: 16577697]
131. Petersen RC, Roberts RO, Knopman DS, Boeve BF, Geda YE, Ivnik RJ, Smith GE, Jack CR. Mild cognitive impairment: ten years later. Arch Neurol. 2009; 66:1447–1455. [PubMed: 20008648]
132. Peterson EC, Wang Z, Britz G. Regulation of cerebral blood flow. Int J Vasc Med. 2011; 2011:823525. [PubMed: 21808738]
133. Popa-Wagner A, Buga A-M, Popescu B, Muresanu D. Vascular cognitive impairment, dementia, aging and energy demand. A vicious cycle. J Neural Transm Vienna Austria. 1996; 122(Suppl 1):S47–S54.
134. Putcha D, O'Keefe K, LaViolette P, O'Brien J, Greve D, Rentz DM, Locascio J, Atri A, Sperling R. Reliability of functional magnetic resonance imaging associative encoding memory paradigms in non-demented elderly adults. Hum Brain Mapp. 2011; 32:2027–2044. [PubMed: 21259385]
135. Raichle ME. Circulatory and metabolic correlates of brain function in normal humans. Comprehensive physiology, Supplement 5: Handbook of physiology, the nervous system, higher functions of the brain. 2011:643–674. **(First published in print 1987)**.
136. Raichle ME, MacLeod AM, Snyder AZ, Powers WJ, Gusnard DA, Shulman GL. A default mode of brain function. Proc Natl Acad Sci USA. 2001; 98:676–682. [PubMed: 11209064]
137. Raz N, Lindenberger U, Rodrigue KM, Kennedy KM, Head D, Williamson A, Dahle C, Gerstorf D, Acker JD. Regional brain changes in aging healthy adults: general trends, individual differences and modifiers. Cereb Cortex N Y N 1991. 2005; 15:1676–1689.
138. Rémy F, Mirrashed F, Campbell B, Richter W. Verbal episodic memory impairment in Alzheimer's disease: a combined structural and functional MRI study. NeuroImage. 2005; 25:253–266. [PubMed: 15734360]
139. Ringman JM, O'Neill J, Geschwind D, Medina L, Apostolova LG, Rodriguez Y, Schaffer B, Varpetian A, Tseng B, Ortiz F, Fitten J, Cummings JL, Bartzokis G. Diffusion tensor imaging in preclinical and presymptomatic carriers of familial Alzheimer's disease mutations. Brain J Neurol. 2007; 130:1767–1776.
140. Roe CM, Fagan AM, Grant EA, Hassenstab J, Moulder KL, Maue Dreyfus D, Sutphen CL, Benzinger TLS, Mintun MA, Holtzman DM, Morris JC. Amyloid imaging and CSF biomarkers in predicting cognitive impairment up to 7.5 years later. Neurology. 2013; 80:1784–1791. [PubMed: 23576620]
141. Rombouts SA, Barkhof F, Veltman DJ, Machielsen WC, Witter MP, Bierlaagh MA, Lazeron RH, Valk J, Scheltens P. Functional MR imaging in Alzheimer's disease during memory encoding. AJNR Am J Neuroradiol. 2000; 21:1869–1875. [PubMed: 11110539]
142. Ruitenberg A, den Heijer T, Bakker SLM, van Swieten JC, Koudstaal PJ, Hofman A, Breteler MMB. Cerebral hypoperfusion and clinical onset of dementia: the Rotterdam Study. Ann Neurol. 2005; 57:789–794. [PubMed: 15929050]
143. Ryan NS, Keihaninejad S, Shakespeare TJ, Lehmann M, Crutch SJ, Malone IB, Thornton JS, Mancini L, Hyare H, Yousry T, Ridgway GR, Zhang H, Modat M, Alexander DC, Rossor MN, Ourselin S, Fox NC. Magnetic resonance imaging evidence for presymptomatic change in thalamus and caudate in familial Alzheimer's disease. Brain J Neurol. 2013; 136:1399–1414.
144. Schabel MC, Parker DL. Uncertainty and bias in contrast concentration measurements using spoiled gradient echo pulse sequences. Phys Med Biol. 2008; 53:2345–2373. [PubMed: 18421121]
145. Schmidt R, Schmidt H, Haybaeck J, Loitfelder M, Weis S, Cavalieri M, Seiler S, Enzinger C, Ropele S, Erkinjuntti T, Pantoni L, Scheltens P, Fazekas F, Jellinger K. Heterogeneity in age-related white matter changes. Acta Neuropathol (Berl). 2011; 122:171–185. [PubMed: 21706175]

146. Schmithorst VJ, Hernandez-Garcia L, Vannest J, Rajagopal A, Lee G, Holland SK. Optimized simultaneous ASL and BOLD functional imaging of the whole brain. J Magn Reson Imaging JMRI. 2014; 39:1104–1117. [PubMed: 24115454]

147. Schuff N, Matsumoto S, Kmiecik J, Studholme C, Du A, Ezekiel F, Miller BL, Kramer JH, Jagust WJ, Chui HC, Weiner MW. Cerebral blood flow in ischemic vascular dementia and Alzheimer's disease, measured by arterial spin-labeling magnetic resonance imaging. Alzheimers Dement J Alzheimers Assoc. 2009; 5:454–462.

148. Seeley WW, Crawford RK, Zhou J, Miller BL, Greicius MD. Neurodegenerative diseases target large-scale human brain networks. Neuron. 2009; 62:42–52. [PubMed: 19376066]

149. Sestini S, Castagnoli A, Mansi L. The new FDG brain revolution: the neurovascular unit and the default network. Eur J Nucl Med Mol Imaging. 2010; 37:913–916. [PubMed: 20033155]

150. Sheline YI, Raichle ME. Resting state functional connectivity in preclinical Alzheimer's disease. Biol Psychiatry. 2013; 74:340–347. [PubMed: 23290495]

151. Shulman GL, Fiez JA, Corbetta M, Buckner RL, Miezin FM, Raichle ME, Petersen SE. Common blood flow changes across visual tasks: II. Decreases in cerebral cortex. J Cogn Neurosci. 1997; 9:648–663. [PubMed: 23965122]

152. Sirotin YB, Das A. Anticipatory haemodynamic signals in sensory cortex not predicted by local neuronal activity. Nature. 2009; 457:475–479. [PubMed: 19158795]

153. Small SA, Perera GM, DeLaPaz R, Mayeux R, Stern Y. Differential regional dysfunction of the hippocampal formation among elderly with memory decline and Alzheimer's disease. Ann Neurol. 1999; 45:466–472. [PubMed: 10211471]

154. Smith CD, Andersen AH, Gold BT. Alzheimer's Disease Neuroimaging Initiative. Structural brain alterations before mild cognitive impairment in ADNI: validation of volume loss in a predefined antero-temporal region. J Alzheimers Dis JAD. 2012; 31(Suppl 3):S49–S58. [PubMed: 22460332]

155. Solé-Padullés C, Bartrés-Faz D, Junqué C, Vendrell P, Rami L, Clemente IC, Bosch B, Villar A, Bargalló N, Jurado MA, Barrios M, Molinuevo JL. Brain structure and function related to cognitive reserve variables in normal aging, mild cognitive impairment and Alzheimer's disease. Neurobiol Aging. 2009; 30:1114–1124. [PubMed: 18053618]

156. Sourbron S, Ingrisch M, Siefert A, Reiser M, Herrmann K. Quantification of cerebral blood flow, cerebral blood volume, and blood-brain-barrier leakage with DCE-MRI. Magn Reson Med. 2009; 62:205–217. [PubMed: 19449435]

157. Sourbron SP, Buckley DL. On the scope and interpretation of the Tofts models for DCE-MRI. Magn Reson Med. 2011; 66:735–745. [PubMed: 21384424]

158. Sourbron SP, Buckley DL. Classic models for dynamic contrast-enhanced MRI. NMR Biomed. 2013; 26:1004–1027. [PubMed: 23674304]

159. Sperling RA, Bates JF, Chua EF, Cocchiarella AJ, Rentz DM, Rosen BR, Schacter DL, Albert MS. fMRI studies of associative encoding in young and elderly controls and mild Alzheimer's disease. J Neurol Neurosurg Psychiatry. 2003; 74:44–50. [PubMed: 12486265]

160. Sperling RA, Johnson KA, Doraiswamy PM, Reiman EM, Fleisher AS, Sabbagh MN, Sadowsky CH, Carpenter A, Davis MD, Lu M, Flitter M, Joshi AD, Clark CM, Grundman M, Mintun MA, Skovronsky DM, Pontecorvo MJ. AV45-A05 Study Group. Amyloid deposition detected with florbetapir F 18 ((18)F-AV-45) is related to lower episodic memory performance in clinically normal older individuals. Neurobiol Aging. 2013; 34:822–831. [PubMed: 22878163]

161. Sperling RA, Laviolette PS, O'Keefe K, O'Brien J, Rentz DM, Pihlajamaki M, Marshall G, Hyman BT, Selkoe DJ, Hedden T, Buckner RL, Becker JA, Johnson KA. Amyloid deposition is associated with impaired default network function in older persons without dementia. Neuron. 2009; 63:178–188. [PubMed: 19640477]

162. Sperling R, Greve D, Dale A, Killiany R, Holmes J, Rosas HD, Cocchiarella A, Firth P, Rosen B, Lake S, Lange N, Routledge C, Albert M. Functional MRI detection of pharmacologically induced memory impairment. Proc Natl Acad Sci USA. 2002; 99:455–460. [PubMed: 11756667]

163. Starr JM, Farrall AJ, Armitage P, McGurn B, Wardlaw J. Blood–brain barrier permeability in Alzheimer's disease: a case-control MRI study. Psychiatry Res. 2009; 171:232–241. [PubMed: 19211227]

164. Stern CE, Corkin S, González RG, Guimaraes AR, Baker JR, Jennings PJ, Carr CA, Sugiura RM, Vedantham V, Rosen BR. The hippocampal formation participates in novel picture encoding: evidence from functional magnetic resonance imaging. Proc Natl Acad Sci USA. 1996; 93:8660–8665. [PubMed: 8710927]

165. Stricker NH, Chang Y-L, Fennema-Notestine C, Delano-Wood L, Salmon DP, Bondi MW, Dale AM. Alzheimer's Disease Neuroimaging Initiative. Distinct profiles of brain and cognitive changes in the very old with Alzheimer disease. Neurology. 2011; 77:713–721. [PubMed: 21832223]

166. Sweeney MD, Sagare AP, Zlokovic BV. Cerebrospinal fluid biomarkers of neurovascular dysfunction in mild dementia and Alzheimer's disease. J Cereb Blood Flow Metab Off J Int Soc Cereb Blood Flow Metab. 2015; 35:1055–1068.

167. Taheri S, Gasparovic C, Huisa BN, Adair JC, Edmonds E, Prestopnik J, Grossetete M, Shah NJ, Wills J, Qualls C, Rosenberg GA. Blood–brain barrier permeability abnormalities in vascular cognitive impairment. Stroke J Cereb Circ. 2011; 42:2158–2163.

168. Taheri S, Gasparovic C, Shah NJ, Rosenberg GA. Quantitative measurement of blood–brain barrier permeability in human using dynamic contrast-enhanced MRI with fast T1 mapping. Magn Reson Med. 2011; 65:1036–1042. [PubMed: 21413067]

169. Tambini A, Davachi L. Persistence of hippocampal multivoxel patterns into postencoding rest is related to memory. Proc Natl Acad Sci USA. 2013; 110:19591–19596. [PubMed: 24218550]

170. Tekes A, Mohamed MA, Browner NM, Calhoun VD, Yousem DM. Effect of age on visuomotor functional MR imaging. Acad Radiol. 2005; 12:739–745. [PubMed: 15935972]

171. Thomsen HS, Morcos SK, Almén T, Bellin M-F, Bertolotto M, Bongartz G, Clement O, Leander P, Heinz-Peer G, Reimer P, Stacul F, van der Molen A, Webb JAW. ESUR Contrast Medium Safety Committee. Nephrogenic systemic fibrosis and gadolinium-based contrast media: updated ESUR Contrast Medium Safety Committee guidelines. Eur Radiol. 2013; 23:307–318. [PubMed: 22865271]

172. Thulborn KR, Waterton JC, Matthews PM, Radda GK. Oxygenation dependence of the transverse relaxation time of water protons in whole blood at high field. Biochim Biophys Acta. 1982; 714:265–270. [PubMed: 6275909]

173. Tian P, Teng IC, May LD, Kurz R, Lu K, Scadeng M, Hillman EMC, De Crespigny AJ, D'Arceuil HE, Mandeville JB, Marota JJA, Rosen BR, Liu TT, Boas DA, Buxton RB, Dale AM, Devor A. Cortical depth-specific microvascular dilation underlies laminar differences in blood oxygenation level-dependent functional MRI signal. Proc Natl Acad Sci USA. 2010; 107:15246–15251. [PubMed: 20696904]

174. Tofts PS, Brix G, Buckley DL, Evelhoch JL, Henderson E, Knopp MV, Larsson HB, Lee TY, Mayr NA, Parker GJ, Port RE, Taylor J, Weisskoff RM. Estimating kinetic parameters from dynamic contrast-enhanced T(1)-weighted MRI of a diffusable tracer: standardized quantities and symbols. J Magn Reson Imaging JMRI. 1999; 10:223–232. [PubMed: 10508281]

175. Tondelli M, Wilcock GK, Nichelli P, De Jager CA, Jenkinson M, Zamboni G. Structural MRI changes detectable up to ten years before clinical Alzheimer's disease. Neurobiol Aging. 2012; 33(825):e25–e36.

176. Tosto G, Zimmerman ME, Hamilton JL, Carmichael OT, Brickman AM. Alzheimer's Disease Neuroimaging Initiative. The effect of white matter hyperintensities on neurodegeneration in mild cognitive impairment. Alzheimers Dement J Alzheimers Assoc. 2015

177. Turner R. How much cortex can a vein drain? Downstream dilution of activation-related cerebral blood oxygenation changes. NeuroImage. 2002; 16:1062–1067. [PubMed: 12202093]

178. Umutlu L, Kraff O, Orzada S, Fischer A, Kinner S, Maderwald S, Antoch G, Quick HH, Forsting M, Ladd ME, Lauenstein TC. Dynamic contrast-enhanced renal MRI at 7 Tesla: preliminary results. Invest Radiol. 2011; 46:425–433. [PubMed: 21317791]

179. Uspenskaia O, Liebetrau M, Herms J, Danek A, Hamann GF. Aging is associated with increased collagen type IV accumulation in the basal lamina of human cerebral microvessels. BMC Neurosci. 2004; 5:37. [PubMed: 15387892]

180. Villemagne VL, Burnham S, Bourgeat P, Brown B, Ellis KA, Salvado O, Szoeke C, Macaulay SL, Martins R, Maruff P, Ames D, Rowe CC, Masters CL. Australian Imaging Biomarkers and

Lifestyle (AIBL) Research Group. Amyloid β deposition, neurodegeneration, and cognitive decline in sporadic Alzheimer's disease: a prospective cohort study. Lancet Neurol. 2013; 12:357–367. [PubMed: 23477989]

181. Villemagne VL, Pike KE, Chételat G, Ellis KA, Mulligan RS, Bourgeat P, Ackermann U, Jones G, Szoeke C, Salvado O, Martins R, O'Keefe G, Mathis CA, Klunk WE, Ames D, Masters CL, Rowe CC. Longitudinal assessment of Aβ and cognition in aging and Alzheimer disease. Ann Neurol. 2011; 69:181–192. [PubMed: 21280088]
182. Viswanathan A, Greenberg SM. Cerebral amyloid angiopathy in the elderly. Ann Neurol. 2011; 70:871–880. [PubMed: 22190361]
183. Wagner AD, Schacter DL, Rotte M, Koutstaal W, Maril A, Dale AM, Rosen BR, Buckner RL. Building memories: remembering and forgetting of verbal experiences as predicted by brain activity. Science. 1998; 281:1188–1191. [PubMed: 9712582]
184. Wahlund LO, Bronge L. Contrast-enhanced MRI of white matter lesions in patients with blood–brain barrier dysfunction. Ann N Y Acad Sci. 2000; 903:477–481. [PubMed: 10818541]
185. Wang H, Golob EJ, Su M-Y. Vascular volume and blood–brain barrier permeability measured by dynamic contrast enhanced MRI in hippocampus and cerebellum of patients with MCI and normal controls. J Magn Reson Imaging JMRI. 2006; 24:695–700. [PubMed: 16878309]
186. Wang L, Kittaka M, Sun N, Schreiber SS, Zlokovic BV. Chronic nicotine treatment enhances focal ischemic brain injury and depletes free pool of brain microvascular tissue plasminogen activator in rats. J Cereb Blood Flow Metab Off J Int Soc Cereb Blood Flow Metab. 1997; 17:136–146.
187. Wang L, Zang Y, He Y, Liang M, Zhang X, Tian L, Wu T, Jiang T, Li K. Changes in hippocampal connectivity in the early stages of Alzheimer's disease: evidence from resting state fMRI. NeuroImage. 2006; 31:496–504. [PubMed: 16473024]
188. Wardlaw JM, Smith EE, Biessels GJ, Cordonnier C, Fazekas F, Frayne R, Lindley RI, O'Brien JT, Barkhof F, Benavente OR, Black SE, Brayne C, Breteler M, Chabriat H, Decarli C, de Leeuw F-E, Doubal F, Duering M, Fox NC, Greenberg S, Hachinski V, Kilimann I, Mok V, van Oostenbrugge R, Pantoni L, Speck O, Stephan BCM, Teipel S, Viswanathan A, Werring D, Chen C, Smith C, van Buchem M, Norrving B, Gorelick PB, Dichgans M. STandards for ReportIng Vascular changes on nEuroimaging (STRIVE v1). Neuroimaging standards for research into small vessel disease and its contribution to ageing and neurodegeneration. Lancet Neurol. 2013; 12:822–838. [PubMed: 23867200]
189. Weiner MW, Veitch DP, Aisen PS, Beckett LA, Cairns NJ, Cedarbaum J, Donohue MC, Green RC, Harvey D, Jack CR, Jagust W, Morris JC, Petersen RC, Saykin AJ, Shaw L, Thompson PM, Toga AW, Trojanowski JQ. Alzheimer's Disease Neuroimaging Initiative. Impact of the Alzheimer's Disease Neuroimaging Initiative, 2004 to 2014. Alzheimers Dement J Alzheimers Assoc. 2015; 11:865–884.
190. Wierenga CE, Bondi MW. Use of functional magnetic resonance imaging in the early identification of Alzheimer's disease. Neuropsychol Rev. 2007; 17:127–143. [PubMed: 17476598]
191. Wierenga CE, Dev SI, Shin DD, Clark LR, Bangen KJ, Jak AJ, Rissman RA, Liu TT, Salmon DP, Bondi MW. Effect of mild cognitive impairment and APOE genotype on resting cerebral blood flow and its association with cognition. J Cereb Blood Flow Metab Off J Int Soc Cereb Blood Flow Metab. 2012; 32:1589–1599.
192. Xu G, Antuono PG, Jones J, Xu Y, Wu G, Ward D, Li S-J. Perfusion fMRI detects deficits in regional CBF during memory-encoding tasks in MCI subjects. Neurology. 2007; 69:1650–1656. [PubMed: 17954780]
193. Yakushev I, Müller MJ, Lorscheider M, Schermuly I, Weibrich C, Dellani PR, Hammers A, Stoeter P, Fellgiebel A. Increased hippocampal head diffusivity predicts impaired episodic memory performance in early Alzheimer's disease. Neuropsychologia. 2010; 48:1447–1453. [PubMed: 20109475]
194. Yassa MA, Stark SM, Bakker A, Albert MS, Gallagher M, Stark CEL. High-resolution structural and functional MRI of hippocampal CA3 and dentate gyrus in patients with amnestic Mild Cognitive Impairment. NeuroImage. 2010; 51:1242–1252. [PubMed: 20338246]

195. Yoshiura T, Hiwatashi A, Yamashita K, Ohyagi Y, Monji A, Takayama Y, Nagao E, Kamano H, Noguchi T, Honda H. Simultaneous measurement of arterial transit time, arterial blood volume, and cerebral blood flow using arterial spin-labeling in patients with Alzheimer disease. AJNR Am J Neuroradiol. 2009; 30:1388–1393. [PubMed: 19342545]

196. Zanto TP, Pa J, Gazzaley A. Reliability measures of functional magnetic resonance imaging in a longitudinal evaluation of mild cognitive impairment. NeuroImage. 2014; 84:443–452. [PubMed: 24018304]

197. Zlokovic BV. Cerebrovascular permeability to peptides: manipulations of transport systems at the blood–brain barrier. Pharm Res. 1995; 12:1395–1406. [PubMed: 8584471]

198. Zlokovic BV. Neurovascular pathways to neurodegeneration in Alzheimer's disease and other disorders. Nat Rev Neurosci. 2011; 12:723–738. [PubMed: 22048062]

199. Zlokovic BV, Begley DJ, Chain-Eliash DG. Blood–brain barrier permeability to leucine-enkephalin, d-alanine2-d-leucine5-enkephalin and their N-terminal amino acid (tyrosine). Brain Res. 1985; 336:125–132. [PubMed: 3891014]

200. Zlokovic BV, Deane R, Sagare AP, Bell RD, Winkler EA. Low-density lipoprotein receptor-related protein-1: a serial clearance homeostatic mechanism controlling Alzheimer's amyloid β-peptide elimination from the brain. J Neurochem. 2010; 115:1077–1089. [PubMed: 20854368]

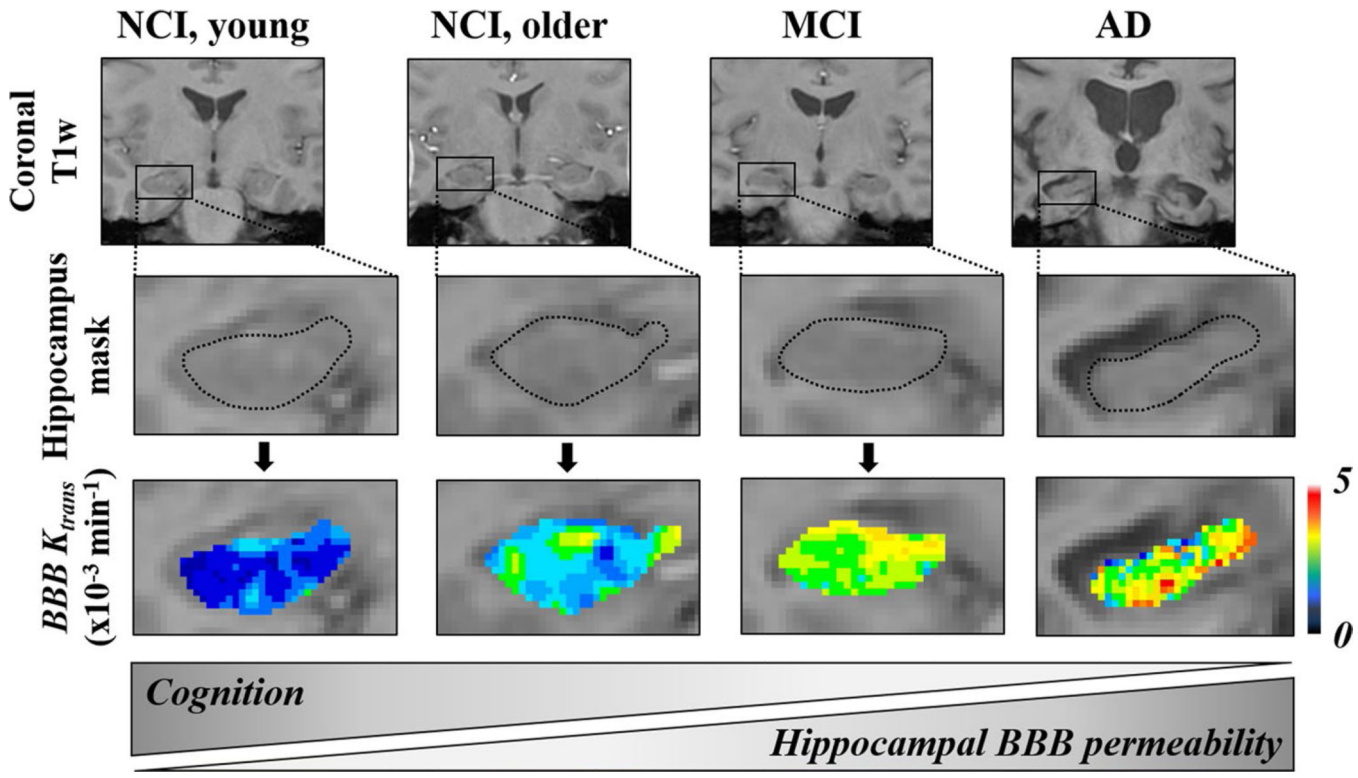

Fig. 1.

BBB breakdown in the hippocampus during normal aging and aging associated with AD using high-resolution DCE-MRI. Representative BBB K_{trans} maps within the left hippocampus in young (23–47 years) and older (55–91 years) individuals with no cognitive impairment (NCI), as well as in older MCI and AD patients (Modified from [115], images courtesy of Axel Montagne)

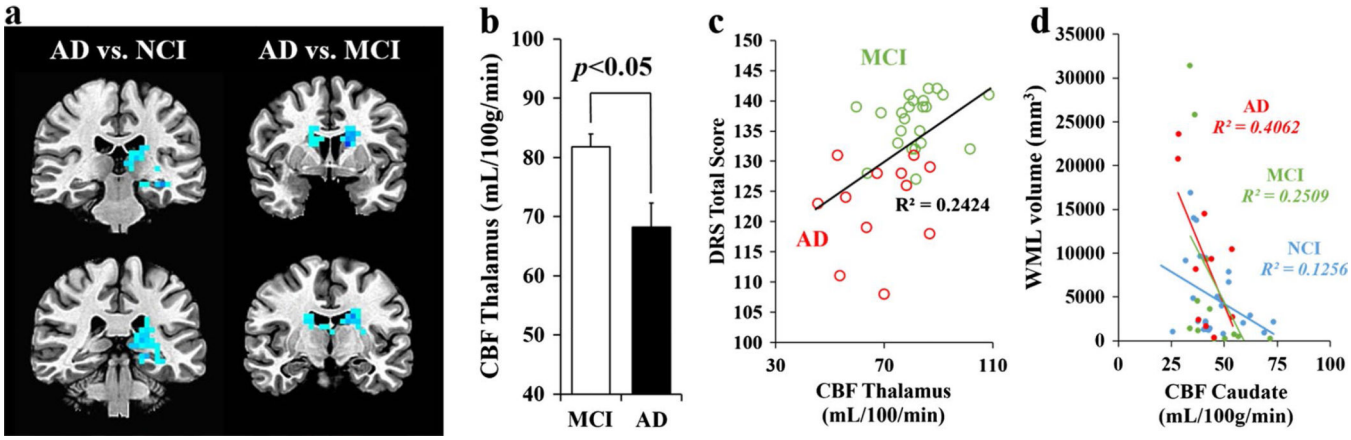

Fig. 2.

Decreases in regional CBF with dementia. **a** Coronal slices display reduced hippocampal, caudate, and thalamic CBF in AD vs. MCI (*right*) and AD vs. no cognitive impairment (NCI) (*left*) groups on voxel-level comparison. **b** The thalamic CBF decreases by 20 % in AD compared to MCI individuals. **c** Thalamic CBF is associated with global cognitive impairment on the Dementia Rating Scale (DRS) in AD (*red*) and MCI (*green*). **d** Caudate CBF reduction is associated with increased white matter lesions (WMLs) severity across the NCI-MCI-AD spectrum. All *p*s < 0.05 after correcting for voxel-level multiple comparisons. NCI, *n* = 46; MCI, *n* = 23; AD, *n* = 12 (Modified from [39, 120]; images courtesy of Daniel Nation)

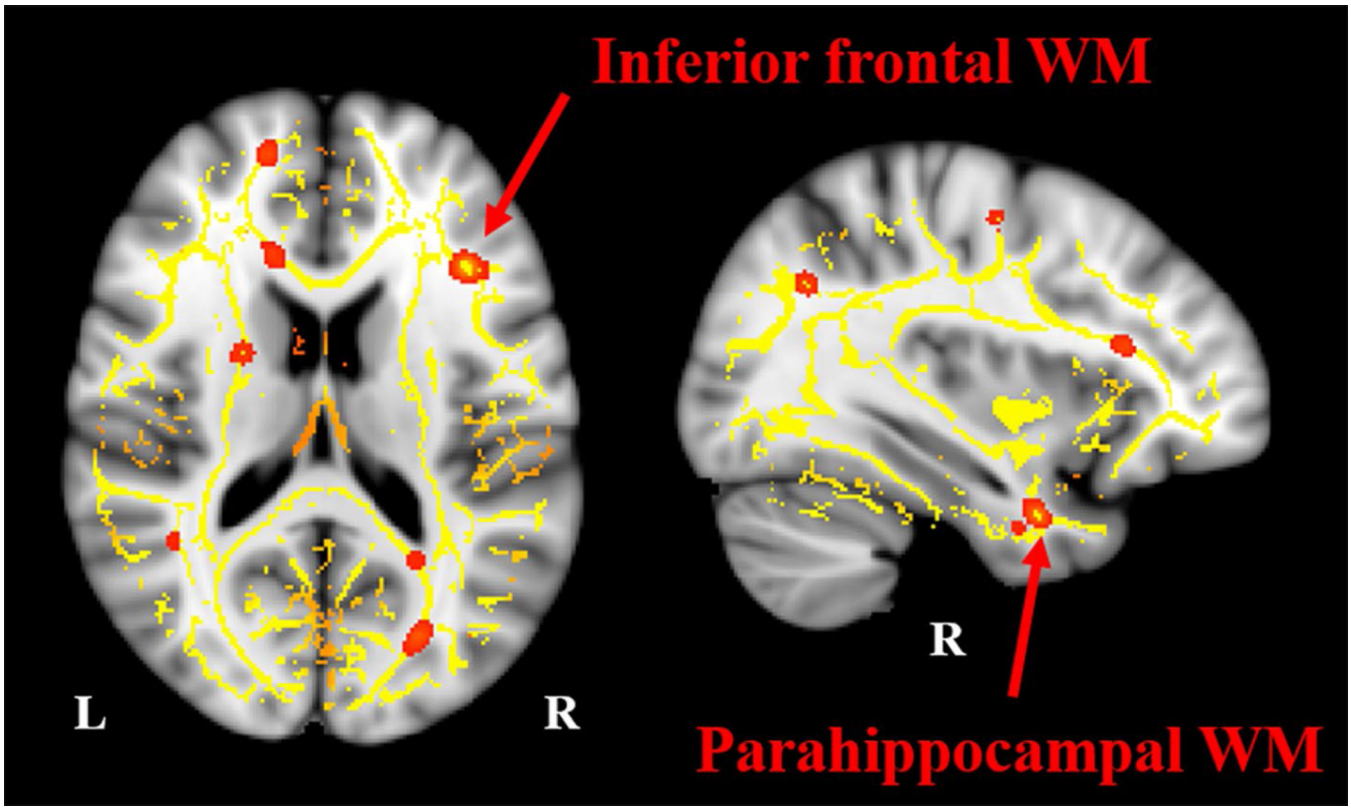

Fig. 3.

White matter disruptions in individuals with MCI. Patients with MCI have lower fractional anisotropy, a measure of white matter (WM) integrity, when compared to cognitively normal older adults ($n = 37$) using tract-based spatial statistics, $p < 0.05$, threshold-free cluster enhancement-corrected for multiple comparisons. The regions *highlighted in red*, including the inferior frontal WM and parahippocampal WM (*red arrows*), may be early sites of damage in individuals at-risk for AD (*L* left; *R* right) (images courtesy of Judy Pa)

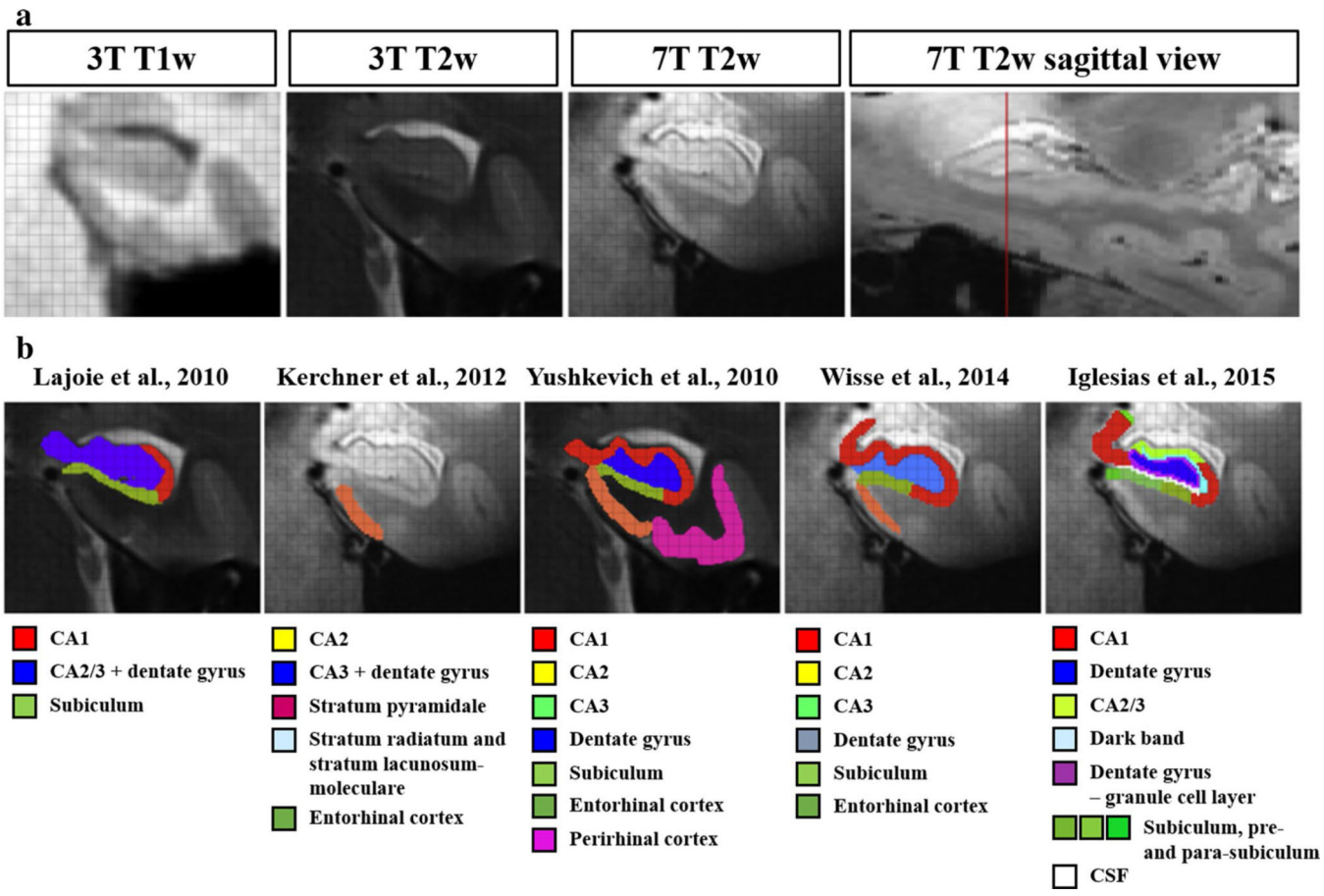

Fig. 4.

Hippocampal subregion segmentation: variations in image acquisition and segmentation protocols. **a** The *figure* shows the left hippocampus of a 36-year-old healthy control acquired with different scanners (3 and 7 T) and sequences [T1-weighted (T1w) and T2w imaging]. Images were segmented by multiple groups (using their own segmentation protocol/atlas) participating in the Hippocampal Subfields Group. Images correspond to the head of the hippocampus. **b** Segmentation examples indicating which substructures were segmented in each protocol (Modified from [62])